A Models Used and Implementation Details

Foundation models. We use 17 foundation models for vision tasks from three categories. They differ in the number of modalities for training (i.e., vision *vs* vision-language), strategy used for training (i.e., contrastive *vs* self-supervised learning), and backbones used (i.e., vision transformers *vs* convolutional neural networks). More conctretely, the DINO (Caron et al., 2021; Oquab et al., 2024) models employed in this work are ViT-based models trained in a self-supervised manner. CLIP (Radford et al., 2021) is a vision-language model, which trains a vision and a text encoder in a contrastive fashion. Last, VICReg (Bardes et al., 2022) are CNNs trained in a self-supervised manner using contrastive learning. Table 4 summarizes the models used for this study.

Implementation details. All linear probing heads are trained with a cross-entropy loss with the Adam (Kingma & Ba, 2017) optimizer and a learning rate of 10^{-4}, whose patience is set to 10. The implementation of the training is based on PyTorch (Paszke et al., 2019), and the conformal predictions methods on TorchCP (Wei & Huang, 2024). For RAPS, we used $k_{\text{RAPS}} = 2$ and $\lambda_{\text{RAPS}} = 0.1$ as hyperparameters. Across all experiments, we use $\alpha = 0.1$, except for CIFAR-10 for which we use $\alpha = 0.05$.

B Relationship Between Model Performance and CP Metrics

Table 5, Table 6, and Table 7 report the numerical values corresponding to Figure 1, showcasing the relationship between the linear probing accuracy of each model, and the CP performance in terms of set size and coverage gap for CIFAR-10, and CIFAR-100, and ImageNet respectively.

C Model Calibration

C.1 Temperature Scaling

We report in Table 8 a more complete version of the results presented in Table 2, containing all explored models.

Additionally, Figures 10, 11, 12, 13, 14, 15, 16, 17, 18 showcase the impact of temperature T on the ECE, set size, minimum class-conditional coverage, and coverage gap across all foundation models. The observations on these figures *strongly align with the findings on the main paper as, regardless of the model, APS yields optimal coverage gap close to the optimal temperature point.* Indeed, looking at the different models (i.e., DINO-based, VICReg and CLIP), we can observe that the behaviour of RAPS (in terms of coverage gap), strongly varies across models. Additionally, Figure 8 shows the evolution of q_α, the threshold on the conformal scores s before and after calibration. When applying temperature scaling, the distribution of softmax across classes approaches a uniform distribution, lowering the scores for the most likely classes. Intuitively, this means that more classes will need to be included in the set to ensure coverage, leading to a decrease in threhsold q_α. This decrease is consistent with the observed increase in set size, which can be seen in Fig. 9, showing the difference in set size when applying temperature scaling for APS on CLIP. Note that this trend holds across models, as a similar behaviour for DINO is observed in Fig. 6 in the main paper. Note that both Fig. 6 and 9 only show cases where the set sizes are different between the calibrated and uncalibrated model.

C.2 Histogram Binning

In Table 9, we explore histogram binning as an alternative method (other than temperature scaling) for model calibration. This method sorts predictions into a predefined number of bins (100 in our case) and adjusts the predictions for the confidence score to match the correct frequency. This is learned on a separate set and applied on a test set. In particular, with this approach as calibration technique we observed an increase in set size, similar to TS, with a slight decrease in MCCC, *aligning with our observations on the effects of calibration on conformalization.*

D Conformal set size analysis

We show the difference between the conformal set size for APS when applied to $\text{ViT}_{\text{ImageNet}}$ and $\text{ViT}_{\text{DINO-S}}$ and for $\text{ViT}_{\text{ImageNet}}$ and $\text{ViT}_{\text{MetaCLIP}}$ in Figure 19, similarly to what is shown in Figure 5.

E Domain Shift

Table 10 reports the numerical values for Fig. 5, showcasing APS's strong performance in terms of marginal and conditional coverage under distribution shift, at the cost of decreasing the set efficiency. Figure 20 depict the distribution of class-conditional coverage for DINOv2-B, VICReg (RN 50x2), and CLIP (ViT-B). The kernel density estimate plots show the class-conditional coverage for a distribution shift with ImageNet-A (*top*), ImageNet-R (*middle*), and ImageNet-V2 (*bottom*), for APS (*left*) and RAPS (*right*). These results clearly demonstrate the stronger resistance to distribution shift for APS compared to RAPS, even when both methods show a minimum class-conditional coverage of 0.

F Few-Shot Adaptation

We present in Table 11 and Table 13 a detailed version of Table 3 for 16 shots, where the *OOD* section (in Table 3) corresponds to the average across all ImageNet variants of Table 11, and the *ID* section corresponds to the average across all 11 datasets of Table 13. Table 12 shows in distribution results for adapting only 4 shots, where we observe slightly higher set size and coverage gap compare to the results for 16 shots.

Table 4: **Summary of the models used.** Models used along with the number of parameters, training scheme, modalities used, and architecture type.

	Num. of parameters	**Training scheme**	**Modalities**	**Architecture**
DINO-S	21,665,664	SSL	Vision	ViT
DINO-B	85,798,656	SSL	Vision	ViT
DINOv2-S	22,056,576	SSL	Vision	ViT
DINOv2-B	86,580,480	SSL	Vision	ViT
DINOv2-L	304,368,640	SSL	Vision	ViT
DINOv2-G	1,136,480,768	SSL	Vision	ViT
VICReg (ResNet-50)	23,508,032	SSL	Vision	CNN
VICReg (ResNet-50x2)	93,907,072	SSL	Vision	CNN
VICReg (ResNet-200x2)	250,128,512	SSL	Vision	CNN
MetaCLIP	149,620,737	Contrastive	Vision-Language	ViT
Phi 3.5	303,507,456	SSL+Supervised	Vision-Language	ViT
LLaVa	303,507,456	SSL+Supervised	Vision-Language	ViT
CLIP (ViT-B)	87,456,000	Contrastive	Vision-Language	ViT
CLIP (ViT-L)	303,966,208	Contrastive	Vision-Language	ViT
CLIP (ViT-H)	632,076,800	Contrastive	Vision-Language	ViT
CLIP (ConvNeXt)	88,221,824	Contrastive	Vision-Language	CNN
CLIP (ConvNeXt-L)	199,770,816	Contrastive	Vision-Language	CNN

Table 5: **Linear probing performance and conformal metrics for CIFAR-10.** Linear probing F1 score, and corresponding set size and MCCC for LAC, APS, and RAPS ($\alpha = 0.05$).

		Set size (↓)			**MCCC** (↑)		
	F1 (↑)	LAC	APS	RAPS	LAC	APS	RAPS
DINO-S	0.8711	1.36 ± 0.00	1.68 ± 0.00	1.53 ± 0.00	0.885 ± 0.001	0.930 ± 0.001	0.913 ± 0.001
DINO-B	0.9165	1.14 ± 0.00	1.41 ± 0.00	1.30 ± 0.00	0.896 ± 0.001	0.932 ± 0.001	0.921 ± 0.001
DINOv2-S	0.9140	1.13 ± 0.00	1.41 ± 0.00	1.29 ± 0.00	0.899 ± 0.001	0.932 ± 0.001	0.927 ± 0.001
DINOv2-B	0.9511	1.01 ± 0.00	1.22 ± 0.00	1.14 ± 0.00	0.899 ± 0.001	0.934 ± 0.001	0.933 ± 0.001
DINOv2-L	0.9848	0.95 ± 0.00	1.03 ± 0.00	1.01 ± 0.00	0.893 ± 0.001	0.933 ± 0.001	0.933 ± 0.001
DINOv2-G	0.9932	0.95 ± 0.00	0.99 ± 0.00	0.98 ± 0.00	0.910 ± 0.001	0.936 ± 0.001	0.934 ± 0.001
VICReg (ResNet-50)	0.8506	1.49 ± 0.00	1.84 ± 0.00	1.69 ± 0.00	0.902 ± 0.001	0.925 ± 0.001	0.905 ± 0.001
VICReg (ResNet-50x2)	0.8749	1.32 ± 0.00	1.65 ± 0.00	1.50 ± 0.00	0.910 ± 0.001	0.930 ± 0.001	0.923 ± 0.001
VICReg (ResNet-200x2)	0.8481	1.47 ± 0.00	1.85 ± 0.00	1.66 ± 0.00	0.907 ± 0.001	0.925 ± 0.001	0.912 ± 0.001
MetaCLIP	0.8926	1.22 ± 0.00	1.59 ± 0.00	1.41 ± 0.00	0.903 ± 0.001	0.933 ± 0.001	0.928 ± 0.001
Phi 3.5	0.8761	1.33 ± 0.00	1.74 ± 0.00	1.51 ± 0.00	0.906 ± 0.001	0.928 ± 0.001	0.921 ± 0.001
LLaVa	0.9159	1.14 ± 0.00	1.46 ± 0.00	1.31 ± 0.00	0.902 ± 0.001	0.935 ± 0.001	0.928 ± 0.001
CLIP (ViT-B)	0.8823	1.33 ± 0.00	1.71 ± 0.00	1.51 ± 0.00	0.909 ± 0.001	0.931 ± 0.001	0.921 ± 0.001
CLIP (ViT-L)	0.9642	0.98 ± 0.00	1.15 ± 0.00	1.09 ± 0.00	0.877 ± 0.001	0.934 ± 0.001	0.932 ± 0.001
CLIP (ViT-H)	0.9519	1.01 ± 0.00	1.26 ± 0.00	1.16 ± 0.00	0.882 ± 0.001	0.933 ± 0.001	0.932 ± 0.001
CLIP (ConvNeXt)	0.8817	1.31 ± 0.00	1.69 ± 0.00	1.49 ± 0.00	0.904 ± 0.001	0.933 ± 0.001	0.922 ± 0.001
CLIP (ConvNeXt-L)	0.9470	1.02 ± 0.00	1.27 ± 0.00	1.18 ± 0.00	0.876 ± 0.001	0.932 ± 0.001	0.932 ± 0.001

Table 6: **Linear probing performance and conformal metrics for CIFAR-100.** Linear probing F1 score, and corresponding set size and MCCC for LAC, APS, and RAPS ($\alpha = 0.1$).

		Set size (↓)			**MCCC** (↑)		
	F1 (↑)	LAC	APS	RAPS	LAC	APS	RAPS
DINO-S	0.6668	3.46 ± 0.01	5.64 ± 0.01	4.29 ± 0.02	0.678 ± 0.003	0.753 ± 0.003	0.682 ± 0.003
DINO-B	0.7379	2.19 ± 0.01	4.07 ± 0.01	2.50 ± 0.01	0.667 ± 0.003	0.772 ± 0.003	0.678 ± 0.003
DINOv2-S	0.7515	2.06 ± 0.01	4.06 ± 0.01	2.40 ± 0.02	0.689 ± 0.004	0.761 ± 0.004	0.700 ± 0.004
DINOv2-B	0.8116	1.39 ± 0.01	3.40 ± 0.01	1.76 ± 0.00	0.671 ± 0.003	0.778 ± 0.003	0.739 ± 0.003
DINOv2-L	0.8885	1.02 ± 0.01	2.37 ± 0.01	1.35 ± 0.00	0.661 ± 0.003	0.779 ± 0.003	0.771 ± 0.002
DINOv2-G	0.9235	0.95 ± 0.00	1.93 ± 0.01	1.21 ± 0.00	0.583 ± 0.004	0.776 ± 0.003	0.762 ± 0.003
VICReg (ResNet-50)	0.6503	3.83 ± 0.01	6.15 ± 0.01	4.83 ± 0.02	0.696 ± 0.004	0.776 ± 0.002	0.702 ± 0.003
VICReg (ResNet-50x2)	0.6902	3.06 ± 0.01	5.30 ± 0.01	3.78 ± 0.01	0.670 ± 0.004	0.771 ± 0.002	0.658 ± 0.004
VICReg (ResNet-200x2)	0.6461	3.95 ± 0.01	6.23 ± 0.02	4.91 ± 0.01	0.713 ± 0.003	0.769 ± 0.002	0.687 ± 0.003
MetaCLIP	0.7015	2.79 ± 0.01	5.25 ± 0.01	3.27 ± 0.01	0.683 ± 0.004	0.769 ± 0.003	0.652 ± 0.003
Phi 3.5	0.6796	3.30 ± 0.01	6.58 ± 0.02	3.94 ± 0.01	0.650 ± 0.004	0.751 ± 0.003	0.654 ± 0.003
LLaVa	0.7201	2.56 ± 0.01	5.31 ± 0.02	2.97 ± 0.01	0.701 ± 0.004	0.762 ± 0.003	0.694 ± 0.003
CLIP (ViT-B)	0.6667	3.52 ± 0.01	6.28 ± 0.02	4.18 ± 0.01	0.705 ± 0.003	0.771 ± 0.002	0.691 ± 0.003
CLIP (ViT-L)	0.8315	1.28 ± 0.00	3.11 ± 0.01	1.67 ± 0.00	0.644 ± 0.003	0.774 ± 0.003	0.738 ± 0.003
CLIP (ViT-H)	0.7973	1.53 ± 0.00	3.79 ± 0.01	1.91 ± 0.00	0.653 ± 0.004	0.761 ± 0.003	0.709 ± 0.004
CLIP (ConvNeXt)	0.6880	3.21 ± 0.00	6.23 ± 0.02	3.99 ± 0.01	0.692 ± 0.003	0.777 ± 0.003	0.648 ± 0.004
CLIP (ConvNeXt-L)	0.7858	1.66 ± 0.00	3.73 ± 0.01	1.97 ± 0.00	0.680 ± 0.004	0.768 ± 0.002	0.714 ± 0.003

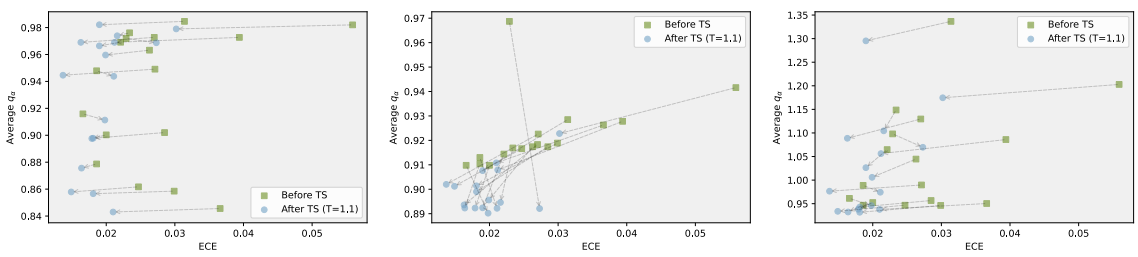

(a) LAC (b) APS (c) RAPS

Figure 8: **ECE and average q_α** threshold before and after calibration for (a) LAC, (b) APS, and (c) RAPS on ImageNet. Each pair represents one model before (*square*) and after (*circle*) calibration.

Table 7: **Linear probing performance and conformal metrics for ImageNet.** Linear probing F1 score, and corresponding set size and MCCC for LAC, APS, and RAPS ($\alpha = 0.1$).

		Set size (↓)			**MCCC** (↑)		
	F1 (↑)	LAC	APS	RAPS	LAC	APS	RAPS
DINO-S	0.7492	3.27 ± 0.01	10.02 ± 0.02	4.23 ± 0.02	0.433 ± 0.005	0.477 ± 0.006	0.412 ± 0.005
DINO-B	0.7743	2.58 ± 0.00	10.73 ± 0.02	3.03 ± 0.00	0.416 ± 0.005	0.521 ± 0.005	0.391 ± 0.005
DINOv2-S	0.7948	1.87 ± 0.00	6.66 ± 0.01	2.12 ± 0.00	0.370 ± 0.006	0.520 ± 0.005	0.384 ± 0.006
DINOv2-B	0.8393	1.36 ± 0.00	7.50 ± 0.02	1.67 ± 0.00	0.414 ± 0.005	0.476 ± 0.005	0.489 ± 0.005
DINOv2-L	0.8624	1.21 ± 0.00	6.77 ± 0.02	1.50 ± 0.00	0.326 ± 0.004	0.502 ± 0.005	0.470 ± 0.004
DINOv2-G	0.8666	1.18 ± 0.00	4.08 ± 0.01	1.44 ± 0.00	0.244 ± 0.005	0.458 ± 0.006	0.350 ± 0.005
VICReg (ResNet-50)	0.7207	4.24 ± 0.01	14.22 ± 0.03	5.73 ± 0.01	0.472 ± 0.004	0.566 ± 0.004	0.453 ± 0.005
VICReg (ResNet-50x2)	0.7570	3.08 ± 0.01	13.49 ± 0.03	3.89 ± 0.01	0.442 ± 0.004	0.549 ± 0.005	0.445 ± 0.004
VICReg (ResNet-200x2)	0.7804	2.50 ± 0.00	12.05 ± 0.03	2.98 ± 0.00	0.440 ± 0.004	0.567 ± 0.004	0.462 ± 0.004
MetaCLIP	0.7580	2.39 ± 0.00	9.43 ± 0.02	2.84 ± 0.00	0.479 ± 0.005	0.535 ± 0.005	0.467 ± 0.004
Phi 3.5	0.7325	2.93 ± 0.00	10.89 ± 0.02	3.50 ± 0.01	0.449 ± 0.005	0.535 ± 0.005	0.464 ± 0.005
LLaVa	0.8500	1.27 ± 0.00	3.83 ± 0.01	1.57 ± 0.00	0.424 ± 0.004	0.537 ± 0.005	0.506 ± 0.005
CLIP (ViT-B)	0.7201	3.03 ± 0.00	9.50 ± 0.02	3.73 ± 0.00	0.434 ± 0.005	0.556 ± 0.004	0.418 ± 0.006
CLIP (ViT-L)	0.8438	1.34 ± 0.00	4.40 ± 0.01	1.66 ± 0.00	0.358 ± 0.006	0.528 ± 0.005	0.462 ± 0.006
CLIP (ViT-H)	0.8393	1.40 ± 0.00	7.85 ± 0.02	1.75 ± 0.00	0.391 ± 0.007	0.553 ± 0.004	0.457 ± 0.006
CLIP (ConvNeXt)	0.7787	2.01 ± 0.00	7.92 ± 0.02	2.28 ± 0.00	0.406 ± 0.007	0.532 ± 0.005	0.454 ± 0.006
CLIP (ConvNeXt-L)	0.8165	1.56 ± 0.00	5.31 ± 0.01	1.88 ± 0.00	0.452 ± 0.006	0.517 ± 0.006	0.456 ± 0.006

Table 8: **Quantitative impact of calibrating vision foundation models with temperature scaling.** Average size and minimum class-conditional coverage are reported between uncalibrated/calibrated models ($T = 1$ and $T = 1.1$ respectively), with ImageNet as benchmark dataset.

	ΔECE	**Set size** (↓)			**MCCC** (↑)		
	($\times 10^{-2}$)	LAC	APS	RAPS	LAC	APS	RAPS
DINO-S	2.57	3.27/3.26	10.02/11.78	4.23/3.99	0.433/0.427	0.477/0.480	0.412/0.415
DINO-B	1.82	2.58/2.55	10.73/13.14	3.03/3.03	0.416/0.398	0.521/0.517	0.391/0.409
DINOv2-S	1.34	1.87/1.87	6.66/8.34	2.12/2.19	0.370/0.351	0.520/0.538	0.384/0.409
DINOv2-B	1.04	1.36/1.36	7.50/10.46	1.67/1.77	0.414/0.406	0.476/0.482	0.489/0.498
DINOv2-L	1.18	1.21/1.21	6.77/9.67	1.50/1.59	0.326/0.336	0.502/0.522	0.453/0.487
DINOv2-G	1.56	1.18/1.18	4.08/5.69	1.44/1.50	0.244/0.243	0.458/0.484	0.350/0.375
VICReg (RN-50)	1.22	4.24/4.19	14.22/16.60	5.73/5.49	0.472/0.468	0.566/0.570	0.453/0.456
VICReg (RN-50x2)	0.18	3.08/3.09	13.49/16.06	3.89/3.80	0.442/0.430	0.549/0.557	0.445/0.446
VICReg (RN-200x2)	0.31	2.50/2.49	12.05/14.61	2.98/3.01	0.440/0.430	0.567/0.566	0.462/0.471
MetaCLIP	0.64	2.39/2.40	9.43/11.31	2.84/2.84	0.479/0.477	0.535/0.541	0.467/0.469
Phi 3.5	-0.44	2.93/2.92	10.89/12.82	3.50/3.38	0.449/0.446	0.535/0.540	0.464/0.468
LLaVa	0.98	1.27/1.27	3.83/4.94	1.57/1.63	0.424/0.426	0.537/0.554	0.506/0.517
CLIP (ViT-B)	1.07	3.03/3.01	9.50/11.11	3.73/3.53	0.434/0.441	0.556/0.564	0.418/0.414
CLIP (ViT-L)	0.22	1.34/1.34	4.40/5.68	1.66/1.74	0.358/0.368	0.528/0.546	0.462/0.470
CLIP (ViT-H)	0.21	1.40/1.41	7.85/9.55	1.75/1.83	0.391/0.392	0.553/0.584	0.457/0.470
CLIP (ConvNeXt)	-0.25	2.01/2.01	7.92/9.74	2.28/2.36	0.406/0.406	0.532/0.560	0.454/0.461
CLIP (ConvNeXt-L)	-0.22	1.56/1.56	5.31/6.69	1.88/1.96	0.452/0.450	0.517/0.542	0.456/0.476

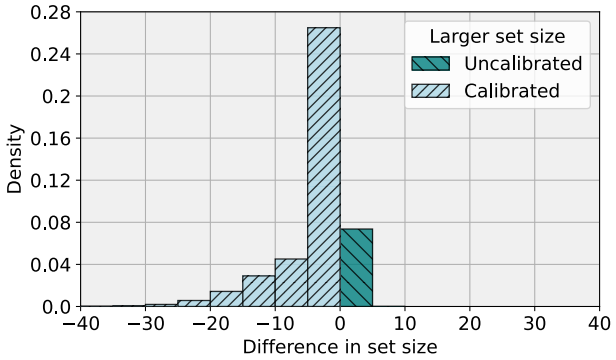

Figure 9: **Difference in conformal set size** (i.e., *efficiency*) when applying temperature scaling ($T = 1.1$) on APS and CLIP (ViT-B).

Table 9: **Quantitative impact of calibrating vision foundation models with histogram binning.** Average size and minimum class-conditional coverage are reported between uncalibrated/calibrated models, with ImageNet as benchmark dataset.

	ΔECE	**AvgSize** (↓)			**MCCC** (↑)		
	($\times 10^{-2}$)	LAC	APS	RAPS	LAC	APS	RAPS
DINO-S	5.59	3.27/135.41	10.02/312.12	4.23/312.15	0.433/0.422	0.477/0.375	0.412/0.375
DINO-B	3.94	2.58/101.94	10.73/269.62	3.03/269.67	0.416/0.417	0.521/0.388	0.391/0.388
DINOv2-S	2.71	1.87/63.19	6.66/186.38	2.12/186.44	0.370/0.427	0.520/0.404	0.384/0.404
DINOv2-B	2.85	1.36/27.33	7.50/87.56	1.67/87.68	0.414/0.372	0.476/0.414	0.489/0.414
DINOv2-L	2.99	1.21/8.86	6.77/31.93	1.50/32.06	0.326/0.311	0.502/0.391	0.453/0.391
DINOv2-G	3.66	1.18/6.25	4.08/20.88	1.44/20.98	0.244/0.280	0.458/0.386	0.350/0.385
VICReg (RN-50)	3.14	4.24/161.07	14.22/374.82	5.73/374.84	0.472/0.456	0.566/0.362	0.453/0.362
VICReg (RN-50x2)	2.34	3.08/130.26	13.49/322.95	3.89/323.00	0.442/0.450	0.549/0.397	0.445/0.397
VICReg (RN-200x2)	2.21	2.50/101.10	12.05/268.30	2.98/268.37	0.440/0.444	0.567/0.384	0.462/0.384
MetaCLIP	2.63	2.39/110.80	9.43/286.46	2.84/286.51	0.479/0.446	0.535/0.396	0.467/0.396
Phi 3.5	2.29	2.93/140.27	10.89/329.86	3.50/329.87	0.449/0.456	0.535/0.384	0.464/0.385
LLaVa	2.47	1.27/13.72	3.83/47.75	1.57/47.87	0.424/0.380	0.537/0.401	0.506/0.402
CLIP (ViT-B)	2.70	3.03/148.29	9.50/337.35	3.73/337.35	0.434/0.458	0.556/0.374	0.418/0.374
CLIP (ViT-L)	1.86	1.34/24.29	4.40/74.14	1.66/74.21	0.358/0.402	0.528/0.418	0.462/0.418
CLIP (ViT-H)	2.00	1.40/30.29	7.85/99.07	1.75/99.19	0.391/0.405	0.553/0.427	0.457/0.427
CLIP (ConvNeXt)	1.86	2.01/84.08	7.92/231.47	2.28/231.52	0.406/0.449	0.532/0.407	0.454/0.407
CLIP (ConvNeXt-L)	1.66	1.56/42.62	5.31/139.04	1.88/139.14	0.452/0.435	0.517/0.413	0.456/0.413

Table 10: **Evaluation under domain-shift.** Set size (↓), coverage (↑), and MCCC (↑) across three CP methods and three foundation models.

		Set size (↓)			**Coverage** (↑)			**MCCC** (↑)		
		LAC	APS	RAPS	LAC	APS	RAPS	LAC	APS	RAPS
ImageNet	DINOv2-B	1.36 ± 0.00	7.50 ± 0.02	1.67 ± 0.00	0.900 ± 0.000	0.900 ± 0.000	0.900 ± 0.000	0.414 ± 0.005	0.476 ± 0.005	0.489 ± 0.005
	VICReg (RN 50x2)	3.08 ± 0.01	13.49 ± 0.02	3.89 ± 0.01	0.900 ± 0.000	0.900 ± 0.000	0.900 ± 0.000	0.442 ± 0.004	0.549 ± 0.005	0.445 ± 0.005
	CLIP (ViT-B)	3.03 ± 0.00	9.50 ± 0.02	3.73 ± 0.00	0.900 ± 0.000	0.901 ± 0.000	0.900 ± 0.000	0.434 ± 0.005	0.556 ± 0.004	0.418 ± 0.006
ImageNet-V2	DINOv2-B	1.38 ± 0.00	9.47 ± 0.04	1.74 ± 0.00	0.879 ± 0.000	0.892 ± 0.000	0.881 ± 0.000	0.081 ± 0.009	0.187 ± 0.009	0.068 ± 0.009
	VICReg (RN 50x2)	3.15 ± 0.00	12.54 ± 0.04	3.89 ± 0.00	0.867 ± 0.000	0.871 ± 0.000	0.870 ± 0.000	0.130 ± 0.008	0.175 ± 0.009	0.143 ± 0.009
	CLIP (ViT-B)	2.88 ± 0.00	6.79 ± 0.02	3.58 ± 0.00	0.877 ± 0.000	0.864 ± 0.000	0.882 ± 0.000	0.023 ± 0.005	0.034 ± 0.007	0.029 ± 0.005
ImageNet-Sketch	DINOv2-B	1.35 ± 0.09	10.90 ± 0.11	1.91 ± 0.31	0.884 ± 0.001	0.904 ± 0.001	0.893 ± 0.001	0.221 ± 0.008	0.322 ± 0.007	0.275 ± 0.007
	VICReg (RN 50x2)	3.49 ± 0.01	21.98 ± 0.05	4.51 ± 0.01	0.826 ± 0.000	0.879 ± 0.000	0.830 ± 0.000	0.119 ± 0.007	0.223 ± 0.008	0.114 ± 0.007
	CLIP (ViT-B)	3.16 ± 0.01	12.98 ± 0.03	3.99 ± 0.01	0.877 ± 0.000	0.900 ± 0.000	0.878 ± 0.000	0.182 ± 0.008	0.293 ± 0.008	0.185 ± 0.007
ImageNet-A	DINOv2-B	1.63 ± 1.76	25.30 ± 1.58	3.55 ± 1.80	0.646 ± 0.001	0.897 ± 0.001	0.734 ± 0.001	0.000 ± 0.010	0.000 ± 0.000	0.000 ± 0.010
	VICReg (RN 50x2)	8.43 ± 0.03	59.83 ± 0.07	7.82 ± 0.01	0.531 ± 0.001	0.879 ± 0.001	0.511 ± 0.001	0.000 ± 0.000	0.000 ± 0.000	0.000 ± 0.000
	CLIP (ViT-B)	6.79 ± 0.02	39.42 ± 0.07	6.45 ± 0.01	0.648 ± 0.001	0.912 ± 0.001	0.624 ± 0.001	0.000 ± 0.000	0.000 ± 0.000	0.000 ± 0.000
ImageNet-R	DINOv2-B	1.31 ± 0.05	7.49 ± 0.04	1.94 ± 0.24	0.867 ± 0.001	0.910 ± 0.001	0.879 ± 0.001	0.282 ± 0.006	0.532 ± 0.009	0.408 ± 0.007
	VICReg (RN 50x2)	5.84 ± 0.02	27.36 ± 0.04	5.65 ± 0.01	0.761 ± 0.001	0.897 ± 0.000	0.742 ± 0.001	0.198 ± 0.007	0.429 ± 0.008	0.186 ± 0.007
	CLIP (ViT-B)	3.38 ± 0.01	11.93 ± 0.03	4.13 ± 0.00	0.893 ± 0.000	0.930 ± 0.000	0.890 ± 0.000	0.422 ± 0.008	0.604 ± 0.007	0.386 ± 0.009

Table 11: **Set size and CovGap** for CLIP (ViT-B) on ImageNet and its variants.

		Set size (↓)			**CovGap** (↓)		
		LAC	APS	RAPS	LAC	APS	RAPS
ImageNet	ZS	2.81 ± 0.00	10.07 ± 0.02	3.23 ± 0.00	0.086 ± 0.000	0.069 ± 0.000	0.084 ± 0.000
	ZSLP	2.17 ± 0.00	6.60 ± 0.01	**2.45** ± 0.00	**0.076** ± 0.000	**0.060** ± 0.000	**0.074** ± 0.000
	CoOp (Zhou et al., 2022b)	2.44 ± 0.00	**6.32** ± 0.01	2.79 ± 0.00	0.080 ± 0.000	0.066 ± 0.000	0.080 ± 0.000
	KgCoOp (Hantao Yao, 2023)	2.47 ± 0.00	7.18 ± 0.01	2.84 ± 0.00	0.081 ± 0.000	0.065 ± 0.000	0.081 ± 0.000
	CLAP (Silva-Rodríguez et al., 2024)	**2.15** ± 0.00	6.83 ± 0.01	**2.45** ± 0.00	0.077 ± 0.000	**0.060** ± 0.000	**0.074** ± 0.000
-V2	ZS	4.64 ± 0.02	17.34 ± 0.08	5.72 ± 0.03	0.128 ± 0.000	0.124 ± 0.000	0.128 ± 0.000
	ZSLP	3.89 ± 0.01	12.51 ± 0.05	4.81 ± 0.01	**0.126** ± 0.000	**0.121** ± 0.000	**0.125** ± 0.000
	CoOp (Zhou et al., 2022b)	4.08 ± 0.01	**11.26** ± 0.06	4.87 ± 0.01	**0.126** ± 0.000	0.123 ± 0.000	0.126 ± 0.000
	KgCoOp (Hantao Yao, 2023)	4.09 ± 0.01	12.65 ± 0.06	4.93 ± 0.02	**0.126** ± 0.000	0.123 ± 0.000	0.126 ± 0.000
	CLAP (Silva-Rodríguez et al., 2024)	**3.72** ± 0.01	12.72 ± 0.05	**4.62** ± 0.01	**0.126** ± 0.000	0.122 ± 0.000	**0.125** ± 0.000
-Sketch	ZS	**14.74** ± 0.02	37.18 ± 0.06	**20.39** ± 0.04	0.099 ± 0.000	**0.090** ± 0.000	0.099 ± 0.000
	ZSLP	16.46 ± 0.03	37.27 ± 0.05	22.79 ± 0.05	**0.098** ± 0.000	0.091 ± 0.000	**0.098** ± 0.000
	CoOp (Zhou et al., 2022b)	16.06 ± 0.03	34.36 ± 0.05	22.12 ± 0.05	**0.098** ± 0.000	0.091 ± 0.000	0.099 ± 0.000
	KgCoOp (Hantao Yao, 2023)	15.46 ± 0.02	**34.35** ± 0.05	21.74 ± 0.04	**0.098** ± 0.000	0.092 ± 0.000	0.099 ± 0.000
	CLAP (Silva-Rodríguez et al., 2024)	15.20 ± 0.03	34.90 ± 0.05	21.29 ± 0.05	**0.098** ± 0.000	**0.090** ± 0.000	**0.098** ± 0.000
-A	ZS	9.42 ± 0.04	16.59 ± 0.06	11.28 ± 0.05	0.094 ± 0.000	0.085 ± 0.000	0.095 ± 0.000
	ZSLP	10.92 ± 0.04	18.63 ± 0.07	12.47 ± 0.05	**0.087** ± 0.000	**0.080** ± 0.000	0.088 ± 0.000
	CoOp (Zhou et al., 2022b)	9.23 ± 0.03	14.65 ± 0.05	10.72 ± 0.05	**0.087** ± 0.001	0.084 ± 0.000	0.090 ± 0.000
	KgCoOp (Hantao Yao, 2023)	**8.66** ± 0.04	**14.39** ± 0.06	**10.19** ± 0.04	0.093 ± 0.000	0.084 ± 0.000	0.096 ± 0.000
	CLAP (Silva-Rodríguez et al., 2024)	9.36 ± 0.03	16.56 ± 0.06	11.38 ± 0.04	**0.087** ± 0.000	0.082 ± 0.000	**0.087** ± 0.000
-R	ZS	**1.92** ± 0.00	5.77 ± 0.01	2.31 ± 0.00	0.059 ± 0.000	**0.039** ± 0.000	0.054 ± 0.000
	ZSLP	2.07 ± 0.00	5.62 ± 0.01	2.36 ± 0.00	**0.058** ± 0.000	0.041 ± 0.000	0.056 ± 0.000
	CoOp (Zhou et al., 2022b)	2.06 ± 0.00	**5.11** ± 0.01	2.40 ± 0.00	0.061 ± 0.000	0.042 ± 0.000	0.063 ± 0.000
	KgCoOp (Hantao Yao, 2023)	1.96 ± 0.00	5.32 ± 0.01	2.29 ± 0.00	0.060 ± 0.000	0.041 ± 0.000	0.058 ± 0.000
	CLAP (Silva-Rodríguez et al., 2024)	**1.92** ± 0.00	5.46 ± 0.01	**2.26** ± 0.01	0.059 ± 0.000	**0.039** ± 0.000	**0.053** ± 0.000

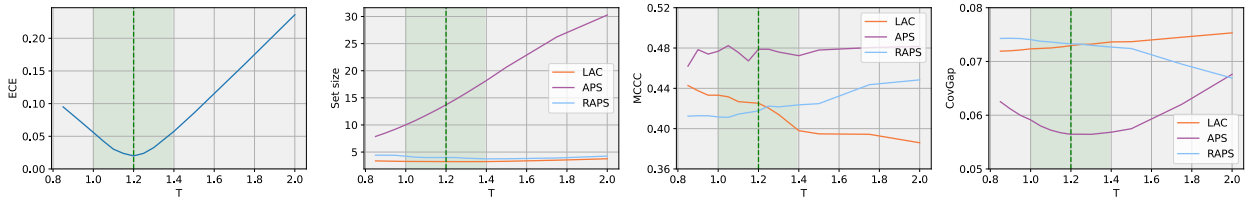

(a) DINO-S

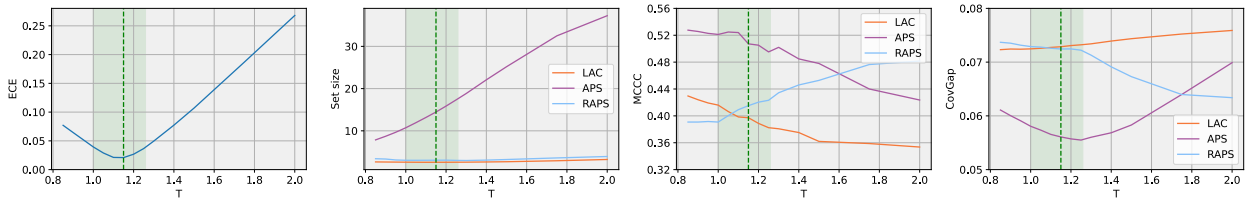

(b) DINO-B

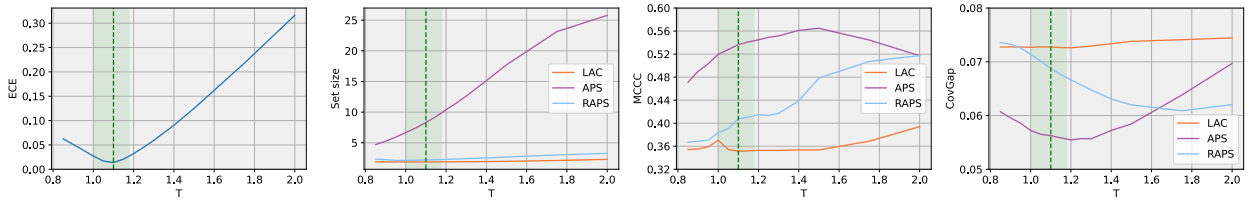

(c) DINOv2-S

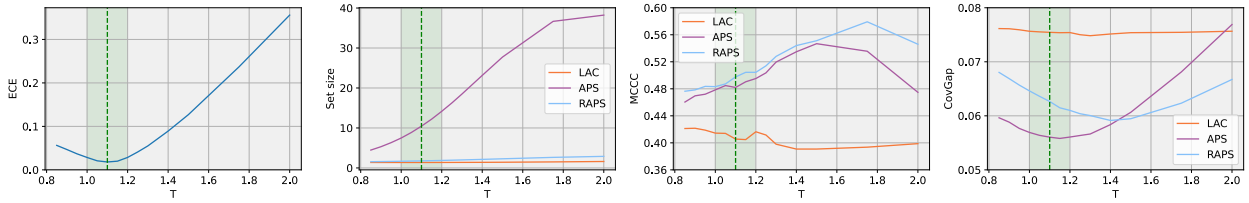

(d) DINOv2-B

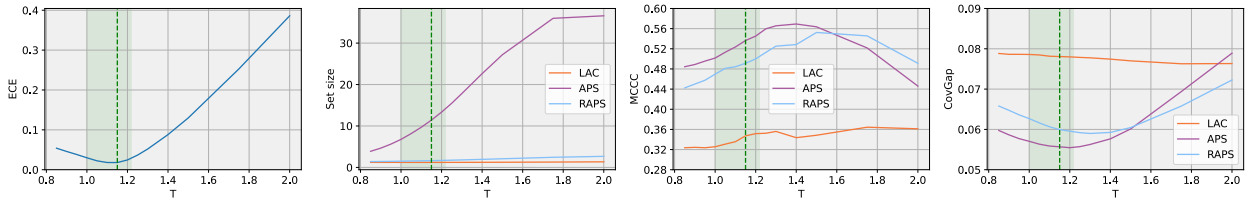

(e) DINOv2-L

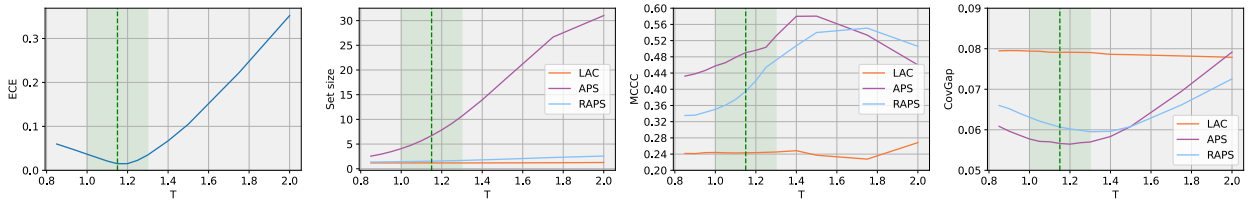

(f) DINOv2-G

Figure 10: **Impact of the temperature T** on the ECE, set size, MCCC, and CovGap, for the DINO and DINOv2 models on ImageNet. $T = 1$ indicates the uncalibrated model performance. Green vertical line indicates the model performance for the optimal temperature.

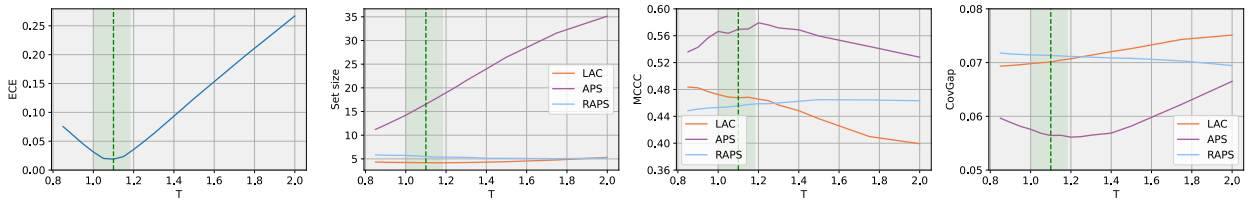

(a) VICReg (ResNet-50)

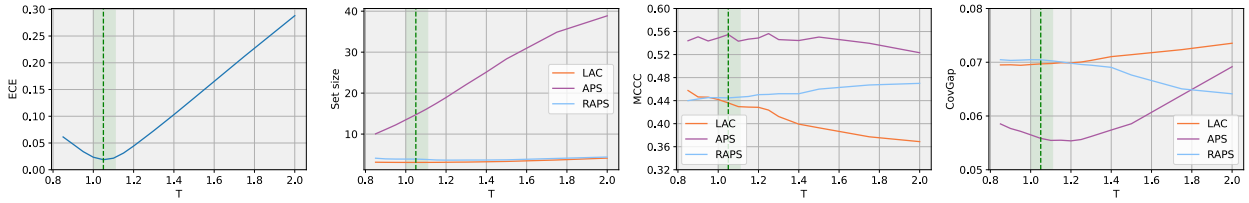

(b) VICReg (ResNet-50x2)

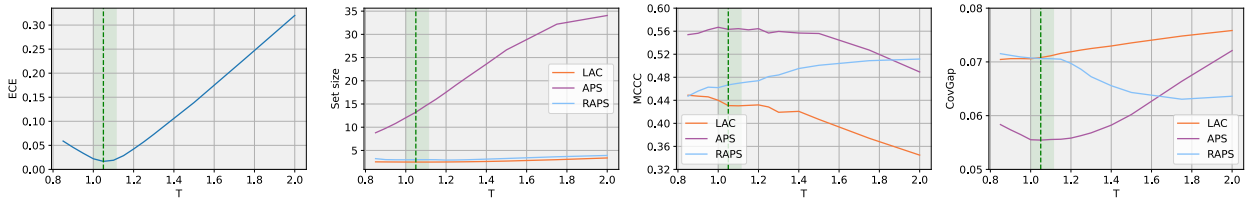

(c) VICReg (ResNet-200x2)

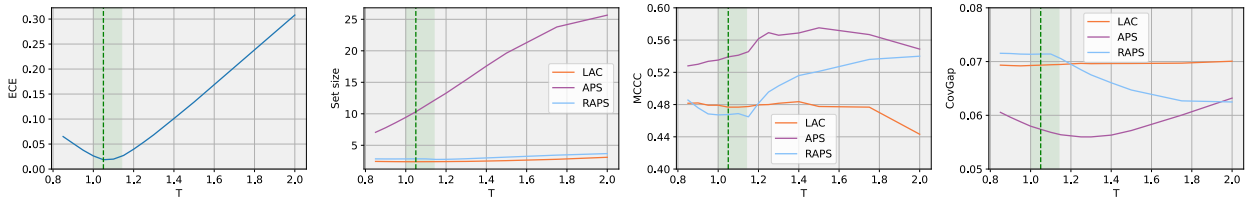

(d) MetaCLIP

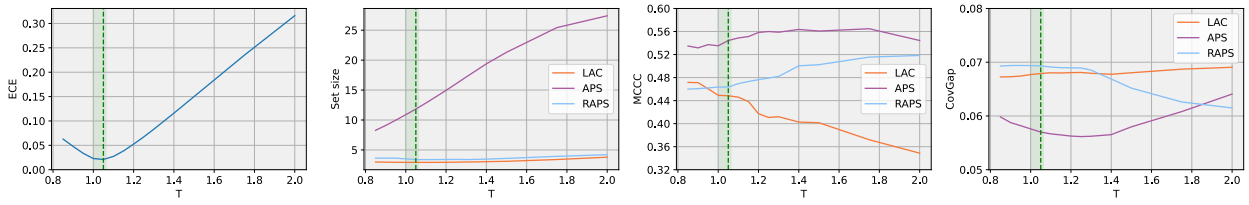

(e) Phi 3.5

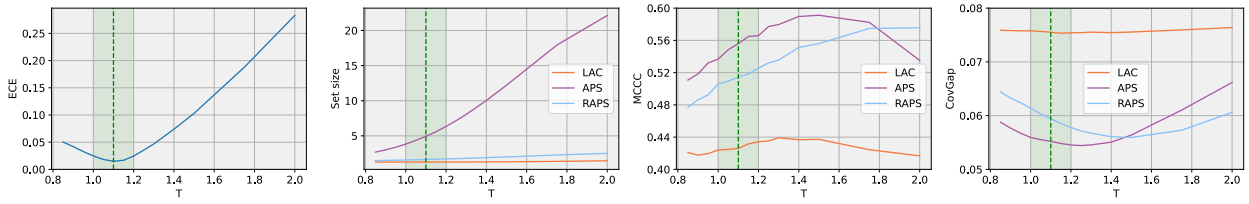

(f) LLaVa

Figure 11: **Impact of the temperature T** on the ECE, set size, MCCC, and CovGap, for the VICReg, MetaCLIP, Phi 3.5 and LLaVa models on ImageNet. $T = 1$ indicates the uncalibrated model performance. Green vertical line indicates the model performance for the optimal temperature.

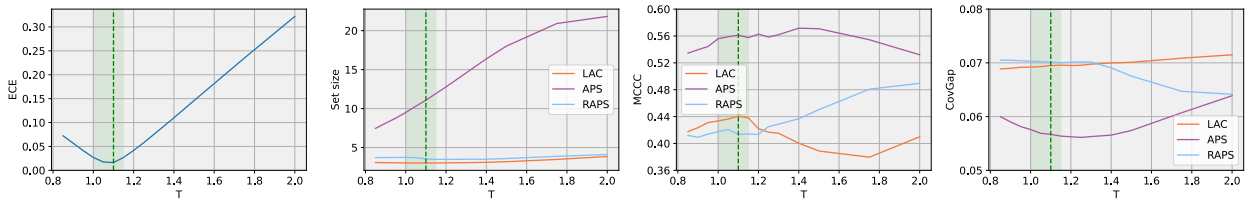

(a) CLIP (ViT-B)

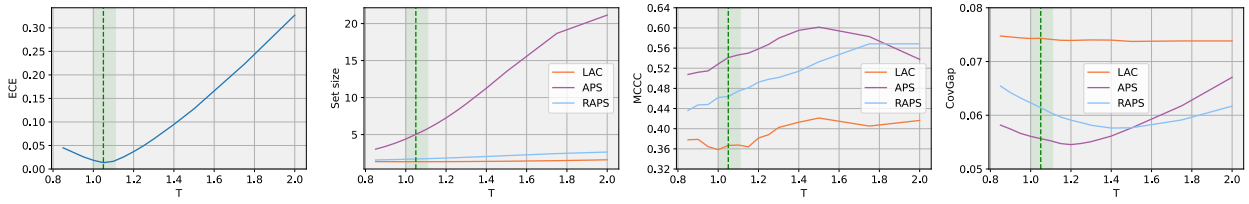

(b) CLIP (ViT-L)

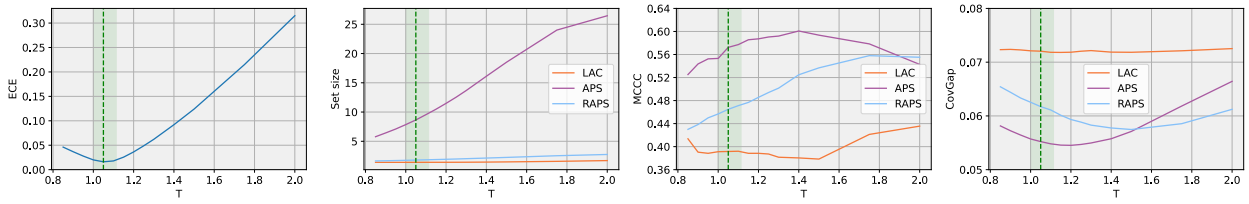

(c) CLIP (ViT-H)

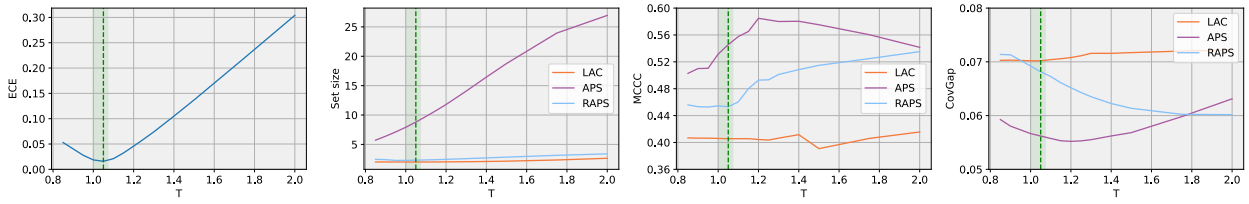

(d) CLIP (ConvNeXt)

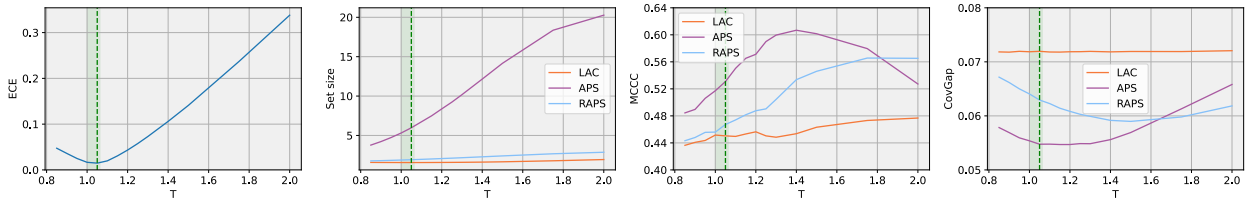

(e) CLIP (ConvNeXt-L)

Figure 12: **Impact of the temperature T** on the ECE, set size, MCCC, and CovGap, for the CLIP models on ImageNet. $T = 1$ indicates the uncalibrated model performance. Green vertical line indicates the model performance for the optimal temperature.

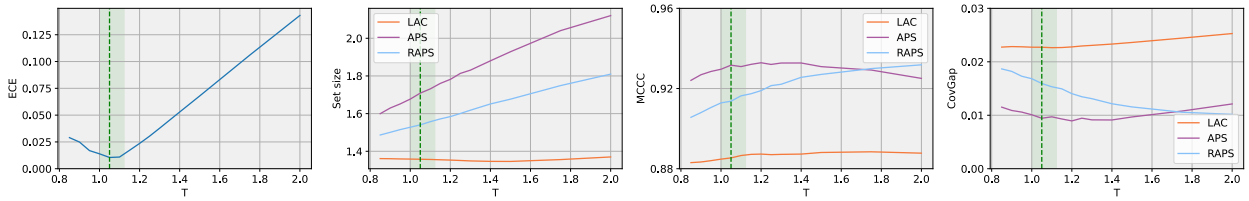

(a) DINO-S

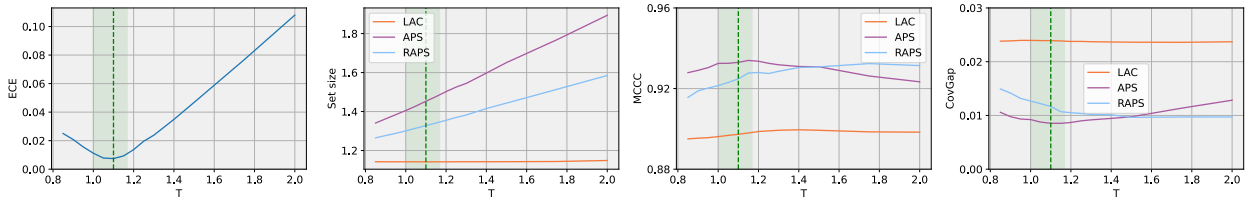

(b) DINO-B

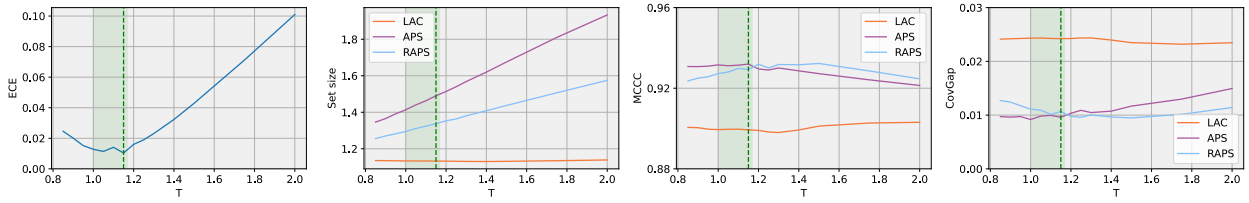

(c) DINOv2-S

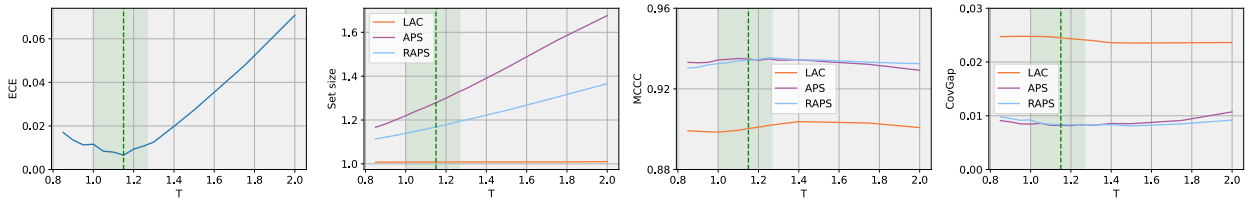

(d) DINOv2-B

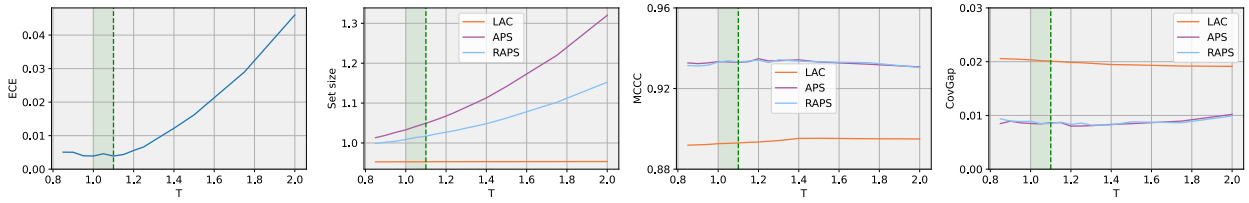

(e) DINOv2-L

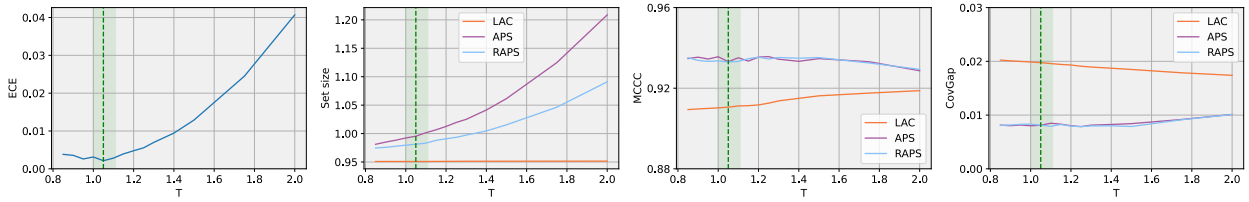

(f) DINOv2-G

Figure 13: **Impact of the temperature T** on the ECE, set size, MCCC, and CovGap, for the DINO and DINOv2 models on CIFAR-10. $T = 1$ indicates the uncalibrated model performance. Green vertical line indicates the model performance for the optimal temperature.

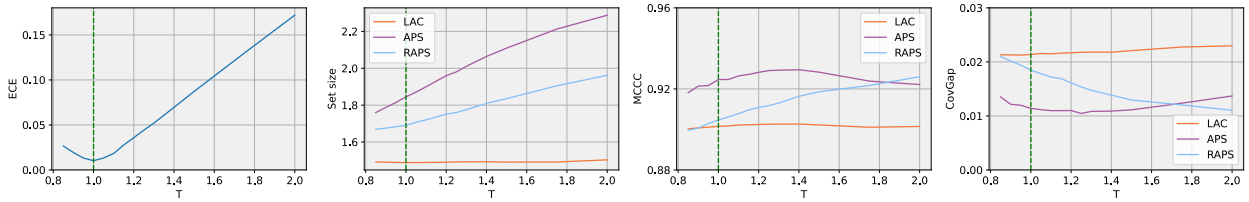

(a) VICReg (ResNet-50)

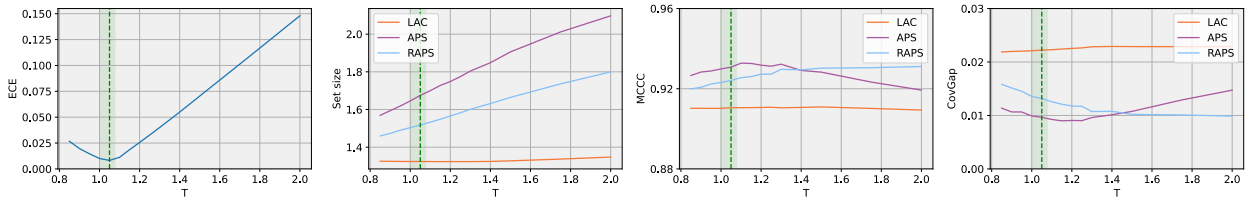

(b) VICReg (ResNet-50x2)

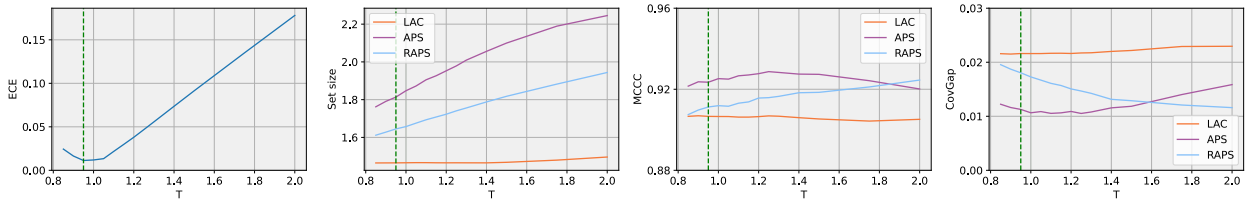

(c) VICReg (ResNet-200x2)

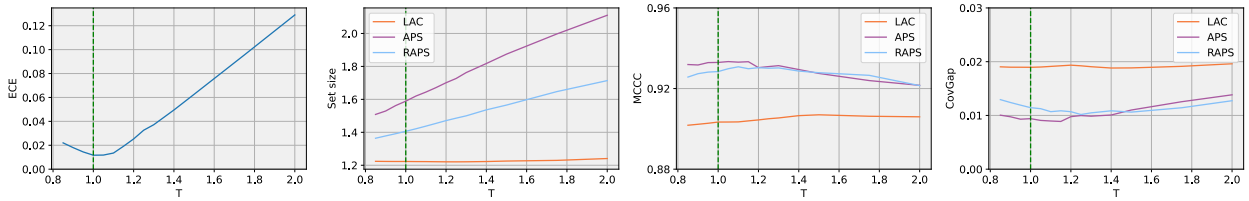

(d) MetaCLIP

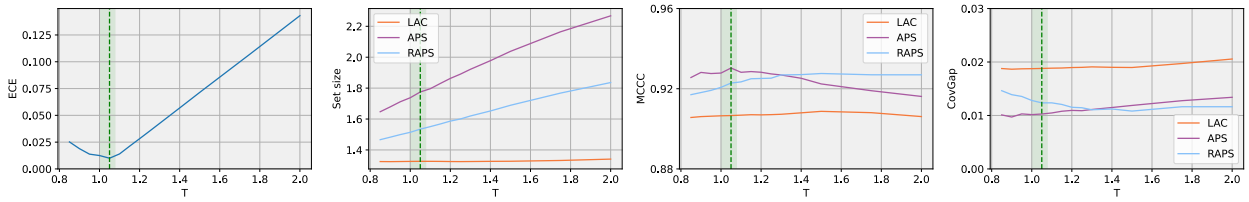

(e) Phi 3.5

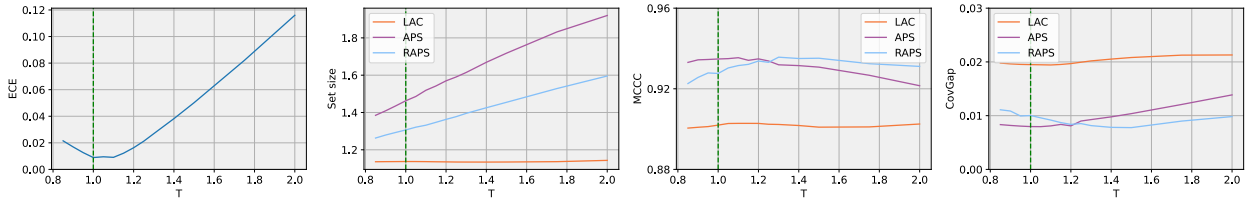

(f) LLaVa

Figure 14: **Impact of the temperature T** on the ECE, set size, MCCC, and CovGap, for the VICReg, MetaCLIP, Phi 3.5 and LLaVa models on CIFAR-10. $T = 1$ indicates the uncalibrated model performance. Green vertical line indicates the model performance for the optimal temperature.

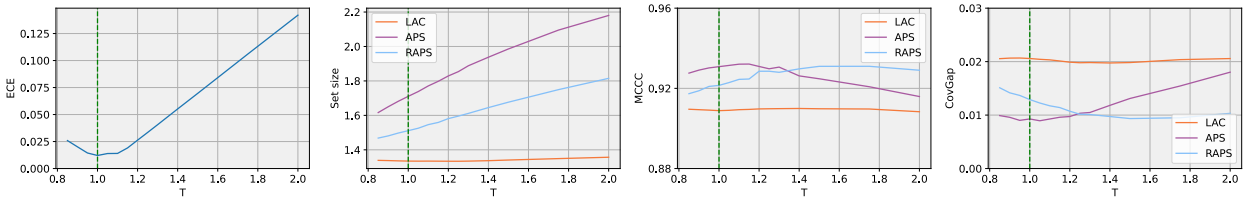

(a) CLIP (ViT-B)

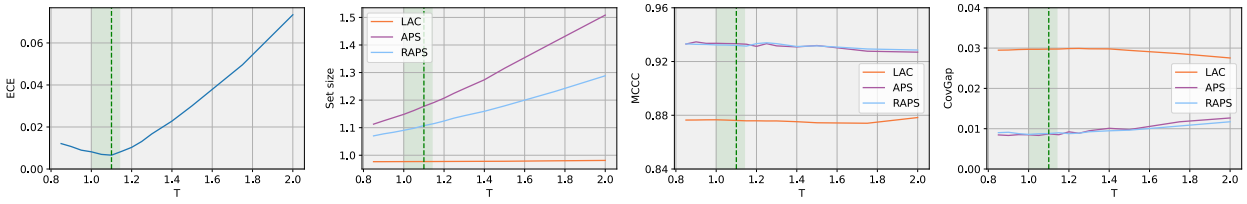

(b) CLIP (ViT-L)

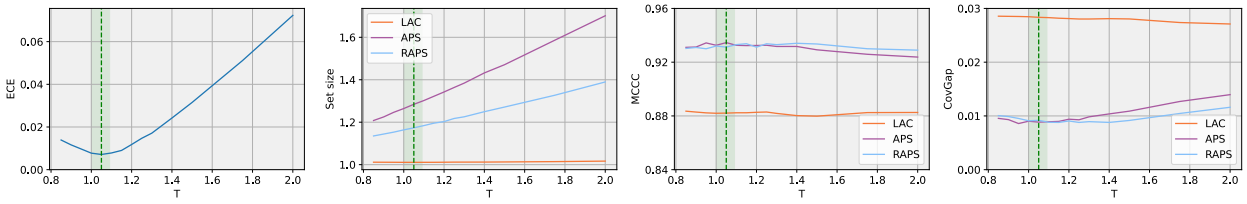

(c) CLIP (ViT-H)

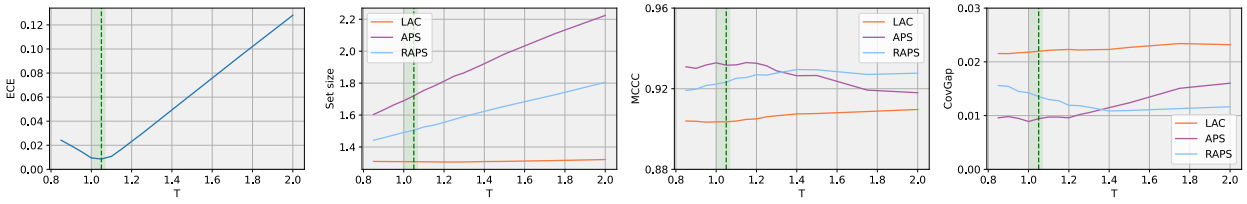

(d) CLIP (ConvNeXt)

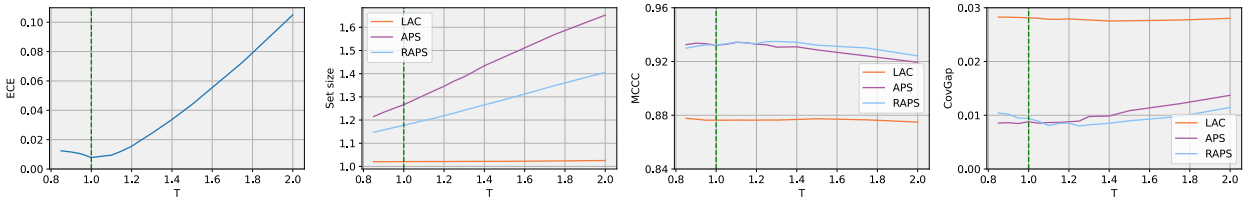

(e) CLIP (ConvNeXt-L)

Figure 15: **Impact of the temperature T** on the ECE, set size, MCCC, and CovGap, for the CLIP models on CIFAR-10. $T = 1$ indicates the uncalibrated model performance. Green vertical line indicates the model performance for the optimal temperature.

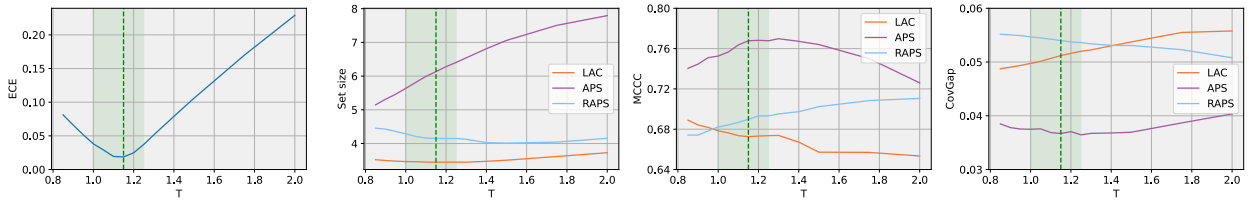

(a) DINO-S

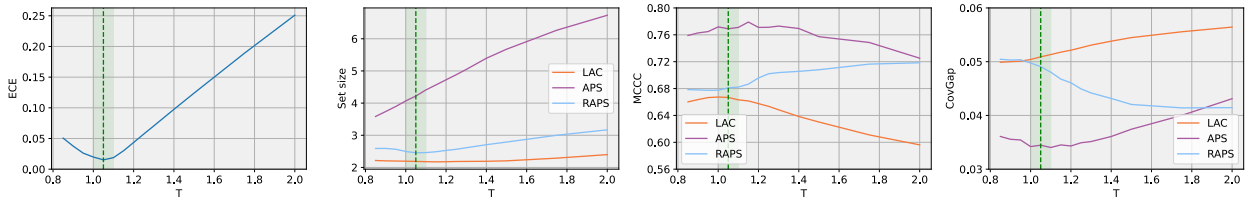

(b) DINO-B

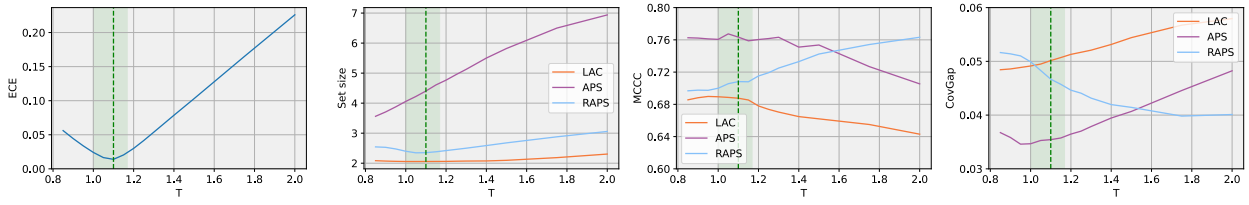

(c) DINOv2-S

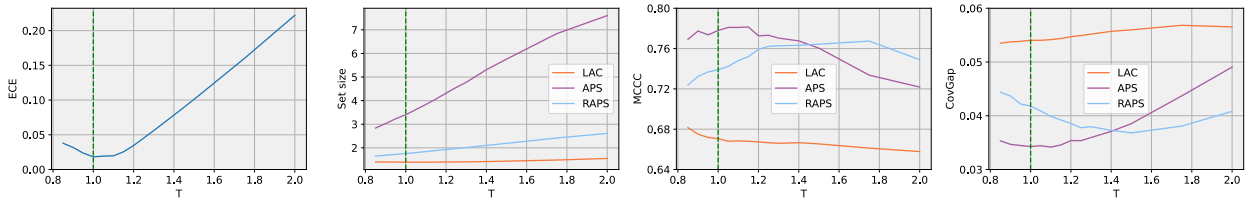

(d) DINOv2-B

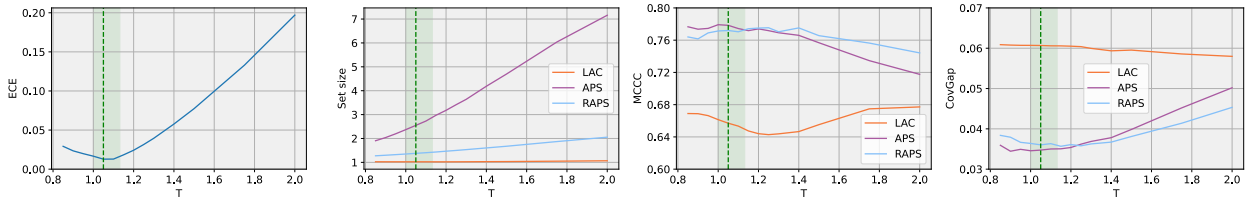

(e) DINOv2-L

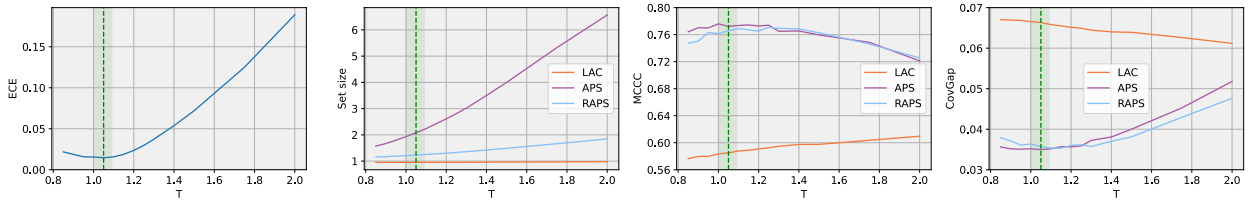

(f) DINOv2-G

Figure 16: **Impact of the temperature T** on the ECE, set size, MCCC, and CovGap, for the DINO and DINOv2 models on CIFAR-100. $T = 1$ indicates the uncalibrated model performance. Green vertical line indicates the model performance for the optimal temperature.

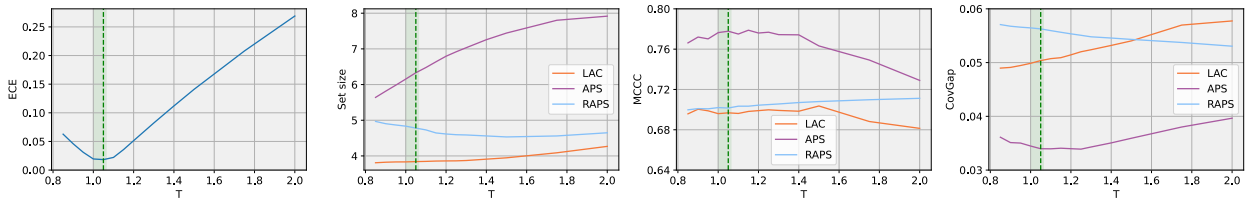

(a) VICReg (ResNet-50)

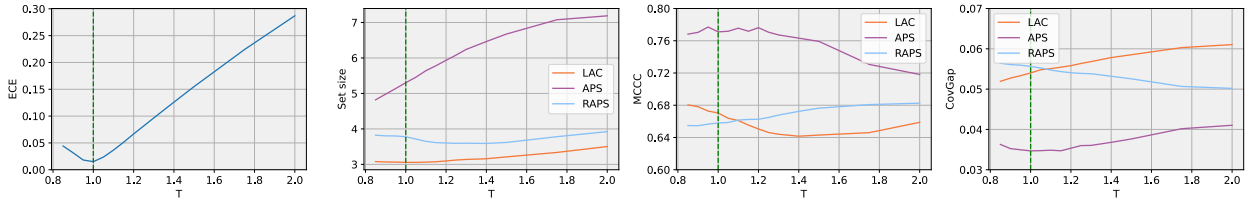

(b) VICReg (ResNet-50x2)

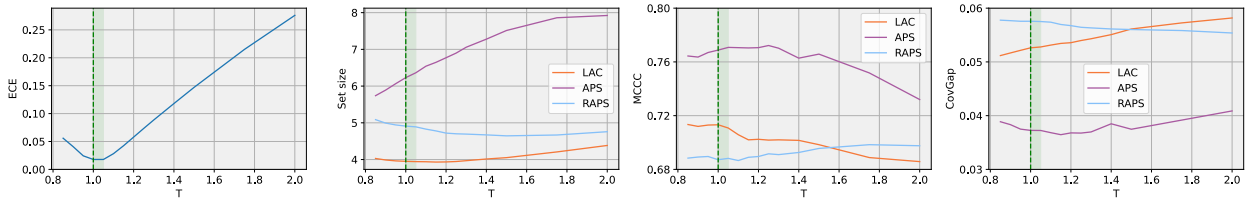

(c) VICReg (ResNet-200x2)

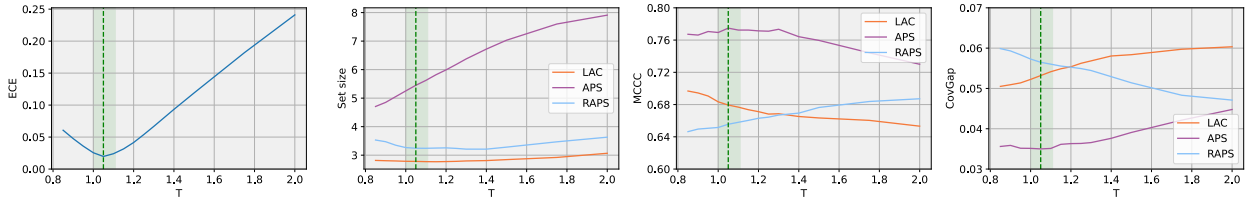

(d) MetaCLIP

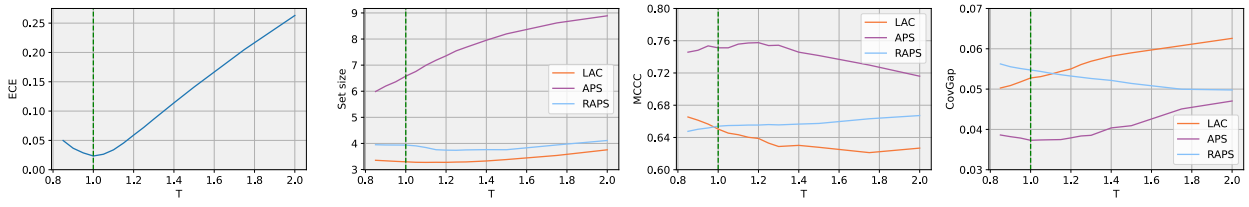

(e) Phi 3.5

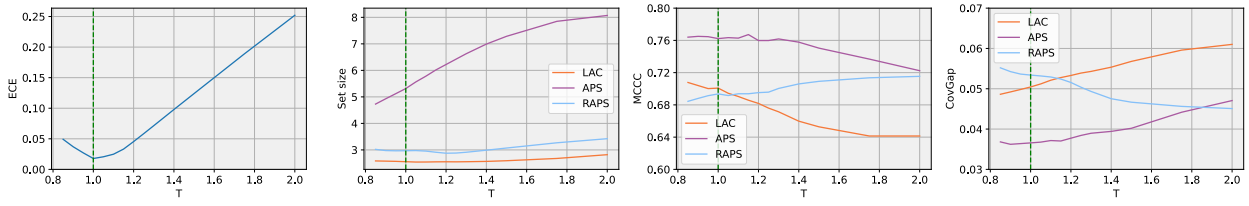

(f) LLaVa

Figure 17: **Impact of the temperature T** on the ECE, set size, MCCC, and CovGap, for the VICReg, MetaCLIP, Phi 3.5 and LLaVa models on CIFAR-100. $T = 1$ indicates the uncalibrated model performance. Green vertical line indicates the model performance for the optimal temperature.

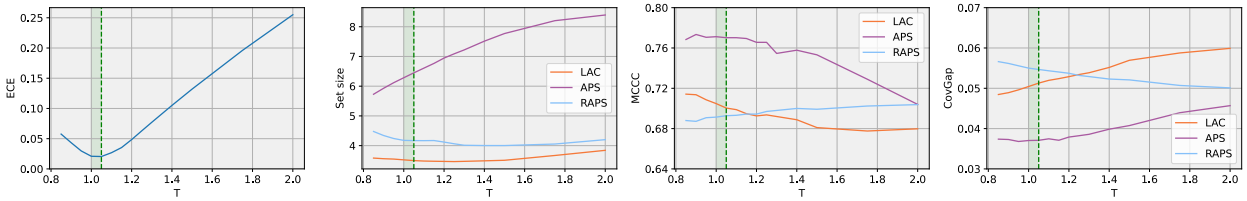

(a) CLIP (ViT-B)

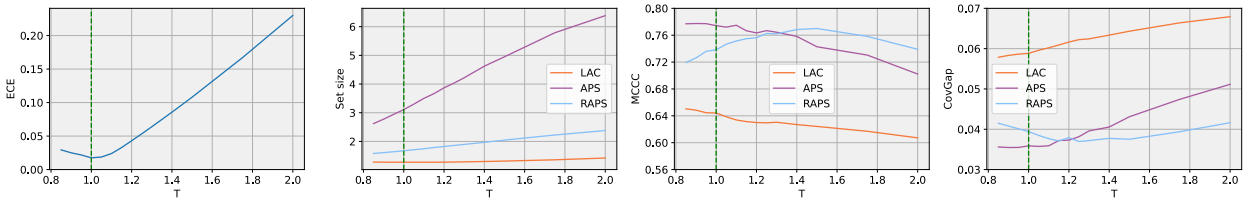

(b) CLIP (ViT-L)

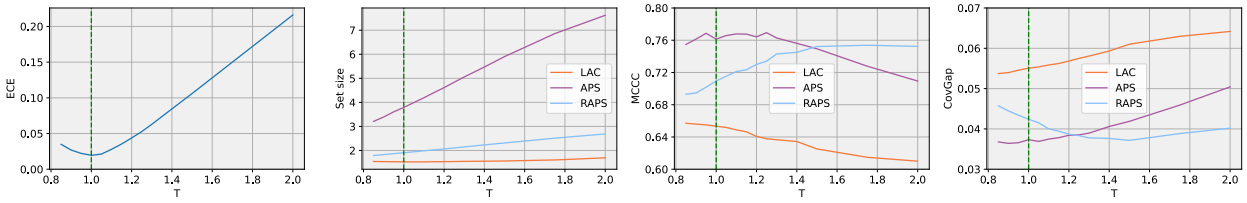

(c) CLIP (ViT-H)

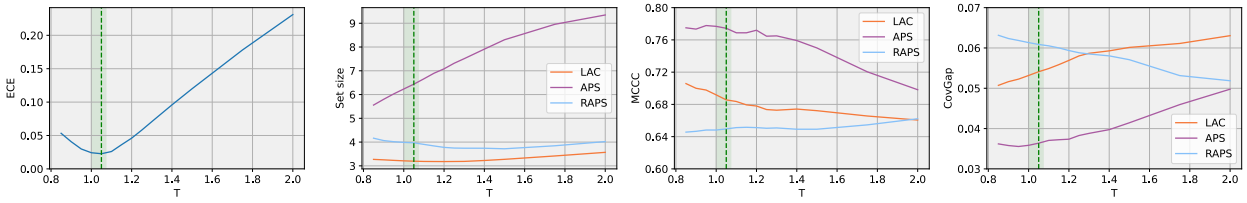

(d) CLIP (ConvNeXt)

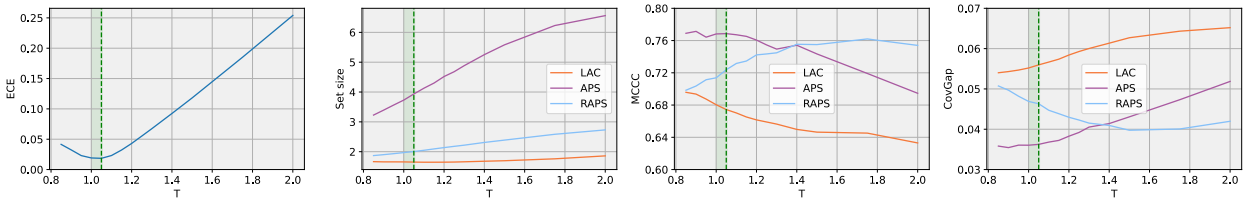

(e) CLIP (ConvNeXt-L)

Figure 18: **Impact of the temperature T** on the ECE, set size, MCCC, and CovGap, for the CLIP models on CIFAR-100. $T = 1$ indicates the uncalibrated model performance. Green vertical line indicates the model performance for the optimal temperature.

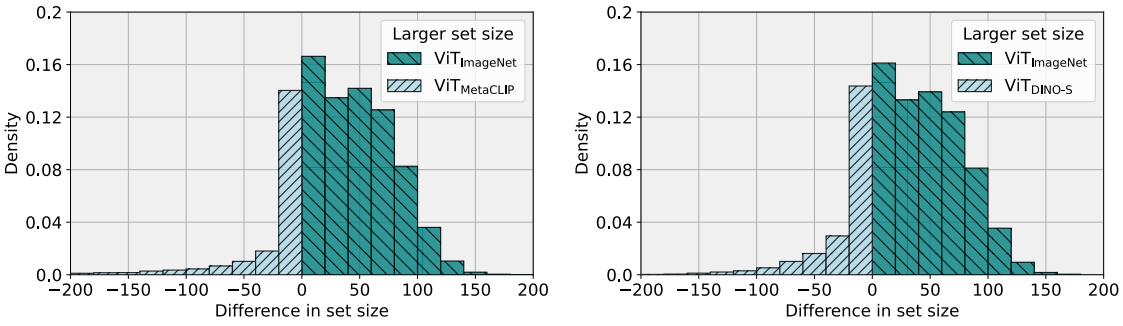

(a) $\text{ViT}_{\text{MetaCLIP}}$ *vs* $\text{ViT}_{\text{ImageNet}}$ (b) $\text{ViT}_{\text{DINO-S}}$ *vs* $\text{ViT}_{\text{ImageNet}}$

Figure 19: **Difference in set size for APS** between (a) $\text{ViT}_{\text{MetaCLIP}}$ and $\text{ViT}_{\text{ImageNet}}$ and between (b) $\text{ViT}_{\text{DINO-S}}$ and $\text{ViT}_{\text{ImageNet}}$. Equal set sizes not shown.

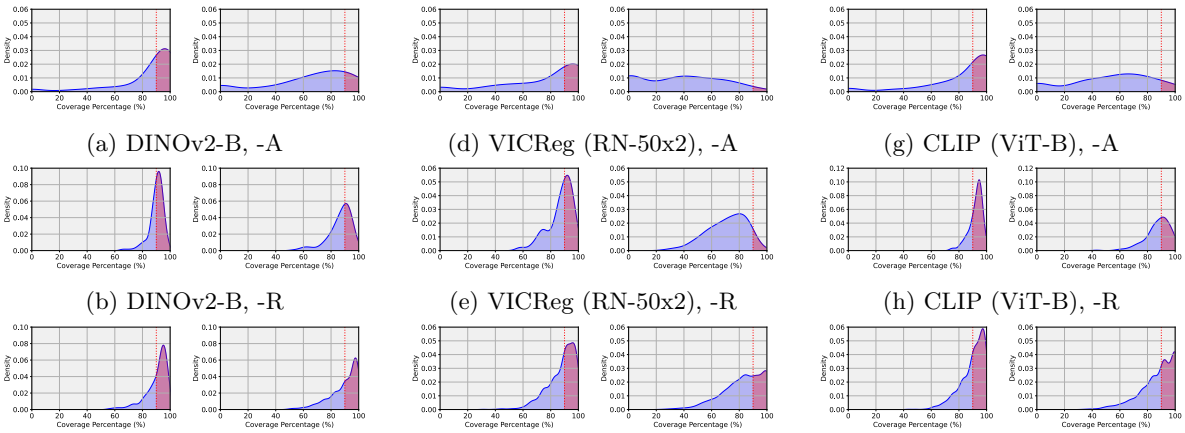

(a) DINOv2-B, -A (d) VICReg (RN-50x2), -A (g) CLIP (ViT-B), -A

(b) DINOv2-B, -R (e) VICReg (RN-50x2), -R (h) CLIP (ViT-B), -R

(c) DINOv2-B, -Sketch (f) VICReg (RN-50x2), -Sketch (i) CLIP (ViT-B), -Sketch

Figure 20: **Domain shift analysis.** Distribution of class-conditional coverages for (a, b, c) DINOv2-B, (d, e, f) VICReg (RN 50x2), and (g, h, i) CLIP (ViT-B). The distribution shift datasets are (a, d, g) ImageNet-A, (b, e, h) ImageNet-R, and (c, f, i) and ImageNet-Sketch. APS (*left*) and RAPS (*right*).

Table 12: **Set size and CovGap** for CLIP (ViT-B) on 11 datasets across several few-shot adaptation approaches. Training for 4 shots.

		Set size (↓)			**CovGap** (↓)		
		LAC	APS	RAPS	LAC	APS	RAPS
Aircraft	ZS	18.70 ± 0.06	19.75 ± 0.06	20.74 ± 0.05	0.138 ± 0.000	0.139 ± 0.000	0.127 ± 0.000
	ZSLP	9.73 ± 0.03	11.13 ± 0.03	11.55 ± 0.05	0.082 ± 0.001	0.073 ± 0.000	0.086 ± 0.001
	CoOp (Zhou et al., 2022b)	9.41 ± 0.03	10.62 ± 0.04	11.38 ± 0.04	0.081 ± 0.001	0.076 ± 0.000	0.088 ± 0.001
	KgCoOp (Hantao Yao, 2023)	9.46 ± 0.03	10.82 ± 0.03	11.00 ± 0.04	0.084 ± 0.001	0.076 ± 0.000	0.086 ± 0.001
	CLAP (Silva-Rodríguez et al., 2024)	9.73 ± 0.03	11.00 ± 0.03	11.51 ± 0.05	0.082 ± 0.001	0.073 ± 0.000	0.086 ± 0.001
Caltech-101	ZS	0.94 ± 0.00	1.95 ± 0.01	1.20 ± 0.00	0.136 ± 0.001	0.092 ± 0.001	0.092 ± 0.001
	ZSLP	0.91 ± 0.00	1.20 ± 0.00	1.05 ± 0.00	0.147 ± 0.001	0.085 ± 0.001	0.085 ± 0.001
	CoOp (Zhou et al., 2022b)	0.92 ± 0.00	1.14 ± 0.00	1.06 ± 0.00	0.143 ± 0.001	0.085 ± 0.001	0.087 ± 0.001
	KgCoOp (Hantao Yao, 2023)	0.92 ± 0.00	1.25 ± 0.00	1.08 ± 0.00	0.147 ± 0.001	0.084 ± 0.001	0.085 ± 0.001
	CLAP (Silva-Rodríguez et al., 2024)	0.91 ± 0.00	1.31 ± 0.01	1.08 ± 0.00	0.144 ± 0.001	0.085 ± 0.001	0.086 ± 0.001
DTD	ZS	11.78 ± 0.06	13.30 ± 0.04	13.66 ± 0.06	0.122 ± 0.001	0.117 ± 0.001	0.121 ± 0.001
	ZSLP	4.74 ± 0.03	6.83 ± 0.03	5.67 ± 0.04	0.092 ± 0.001	0.077 ± 0.001	0.091 ± 0.001
	CoOp (Zhou et al., 2022b)	5.68 ± 0.03	6.46 ± 0.04	7.00 ± 0.05	0.099 ± 0.001	0.093 ± 0.001	0.098 ± 0.001
	KgCoOp (Hantao Yao, 2023)	5.33 ± 0.03	6.22 ± 0.04	6.33 ± 0.05	0.097 ± 0.001	0.083 ± 0.001	0.096 ± 0.001
	CLAP (Silva-Rodríguez et al., 2024)	4.75 ± 0.03	6.83 ± 0.03	5.68 ± 0.04	0.094 ± 0.001	0.079 ± 0.001	0.093 ± 0.001
EuroSAT	ZS	4.55 ± 0.01	4.78 ± 0.00	5.06 ± 0.01	0.103 ± 0.001	0.101 ± 0.001	0.102 ± 0.000
	ZSLP	1.62 ± 0.00	2.22 ± 0.00	1.99 ± 0.00	0.043 ± 0.000	0.051 ± 0.000	0.042 ± 0.000
	CoOp (Zhou et al., 2022b)	1.82 ± 0.00	2.16 ± 0.00	1.95 ± 0.00	0.043 ± 0.000	0.028 ± 0.000	0.034 ± 0.000
	KgCoOp (Hantao Yao, 2023)	1.51 ± 0.00	1.92 ± 0.00	1.76 ± 0.00	0.028 ± 0.000	0.030 ± 0.000	0.032 ± 0.000
	CLAP (Silva-Rodríguez et al., 2024)	1.73 ± 0.00	2.33 ± 0.00	2.06 ± 0.00	0.043 ± 0.000	0.048 ± 0.000	0.041 ± 0.000
Flowers-102	ZS	9.26 ± 0.05	9.52 ± 0.06	15.15 ± 0.08	0.180 ± 0.000	0.175 ± 0.000	0.179 ± 0.000
	ZSLP	1.09 ± 0.00	2.36 ± 0.01	1.65 ± 0.00	0.132 ± 0.001	0.089 ± 0.001	0.095 ± 0.001
	CoOp (Zhou et al., 2022b)	1.13 ± 0.00	1.80 ± 0.01	1.51 ± 0.00	0.104 ± 0.001	0.080 ± 0.001	0.083 ± 0.001
	KgCoOp (Hantao Yao, 2023)	1.19 ± 0.00	2.04 ± 0.01	1.64 ± 0.00	0.114 ± 0.001	0.082 ± 0.001	0.085 ± 0.001
	CLAP (Silva-Rodríguez et al., 2024)	1.15 ± 0.00	2.47 ± 0.01	1.70 ± 0.00	0.137 ± 0.001	0.092 ± 0.001	0.097 ± 0.001
Food-101	ZS	1.14 ± 0.00	1.89 ± 0.00	1.45 ± 0.00	0.054 ± 0.000	0.026 ± 0.000	0.031 ± 0.000
	ZSLP	1.11 ± 0.00	1.82 ± 0.00	1.42 ± 0.00	0.046 ± 0.000	0.023 ± 0.000	0.026 ± 0.000
	CoOp (Zhou et al., 2022b)	1.15 ± 0.00	1.77 ± 0.00	1.41 ± 0.00	0.050 ± 0.000	0.026 ± 0.000	0.030 ± 0.000
	KgCoOp (Hantao Yao, 2023)	1.10 ± 0.00	1.86 ± 0.00	1.43 ± 0.00	0.050 ± 0.000	0.025 ± 0.000	0.027 ± 0.000
	CLAP (Silva-Rodríguez et al., 2024)	1.10 ± 0.00	1.83 ± 0.00	1.42 ± 0.00	0.047 ± 0.000	0.023 ± 0.000	0.026 ± 0.000
ImageNet	ZS	2.81 ± 0.00	10.07 ± 0.02	3.23 ± 0.00	0.086 ± 0.000	0.069 ± 0.000	0.084 ± 0.000
	ZSLP	2.48 ± 0.00	8.02 ± 0.02	2.88 ± 0.00	0.078 ± 0.000	0.062 ± 0.000	0.078 ± 0.000
	CoOp (Zhou et al., 2022b)	2.69 ± 0.00	7.33 ± 0.01	3.03 ± 0.00	0.081 ± 0.000	0.067 ± 0.000	0.081 ± 0.000
	KgCoOp (Hantao Yao, 2023)	2.65 ± 0.00	8.60 ± 0.02	3.01 ± 0.00	0.082 ± 0.000	0.066 ± 0.000	0.082 ± 0.000
	CLAP (Silva-Rodríguez et al., 2024)	2.44 ± 0.00	8.05 ± 0.01	2.82 ± 0.00	0.079 ± 0.000	0.062 ± 0.000	0.079 ± 0.000
Oxford Pets	ZS	1.05 ± 0.00	1.43 ± 0.00	1.33 ± 0.00	0.109 ± 0.000	0.067 ± 0.000	0.072 ± 0.000
	ZSLP	0.95 ± 0.00	1.26 ± 0.00	1.19 ± 0.00	0.080 ± 0.001	0.039 ± 0.000	0.038 ± 0.000
	CoOp (Zhou et al., 2022b)	0.95 ± 0.00	1.17 ± 0.00	1.13 ± 0.00	0.084 ± 0.000	0.036 ± 0.001	0.036 ± 0.001
	KgCoOp (Hantao Yao, 2023)	0.94 ± 0.00	1.20 ± 0.00	1.15 ± 0.00	0.079 ± 0.000	0.038 ± 0.001	0.037 ± 0.001
	CLAP (Silva-Rodríguez et al., 2024)	0.95 ± 0.00	1.28 ± 0.00	1.20 ± 0.00	0.084 ± 0.001	0.039 ± 0.000	0.038 ± 0.000
Cars	ZS	2.24 ± 0.00	3.09 ± 0.01	2.49 ± 0.00	0.109 ± 0.000	0.080 ± 0.000	0.102 ± 0.000
	ZSLP	1.62 ± 0.00	2.39 ± 0.01	1.94 ± 0.00	0.083 ± 0.000	0.061 ± 0.000	0.067 ± 0.000
	CoOp (Zhou et al., 2022b)	1.95 ± 0.00	2.64 ± 0.00	2.21 ± 0.00	0.087 ± 0.000	0.065 ± 0.000	0.078 ± 0.000
	KgCoOp (Hantao Yao, 2023)	1.99 ± 0.00	2.77 ± 0.00	2.29 ± 0.00	0.096 ± 0.000	0.069 ± 0.000	0.084 ± 0.000
	CLAP (Silva-Rodríguez et al., 2024)	1.63 ± 0.00	2.40 ± 0.00	1.96 ± 0.00	0.085 ± 0.000	0.061 ± 0.000	0.067 ± 0.000
SUN397	ZS	2.83 ± 0.01	5.80 ± 0.01	3.21 ± 0.01	0.093 ± 0.000	0.073 ± 0.000	0.093 ± 0.000
	ZSLP	2.00 ± 0.00	3.96 ± 0.01	2.29 ± 0.00	0.080 ± 0.000	0.060 ± 0.000	0.072 ± 0.000
	CoOp (Zhou et al., 2022b)	2.35 ± 0.00	3.76 ± 0.01	2.64 ± 0.00	0.082 ± 0.000	0.068 ± 0.000	0.081 ± 0.000
	KgCoOp (Hantao Yao, 2023)	2.34 ± 0.00	4.18 ± 0.01	2.60 ± 0.00	0.083 ± 0.000	0.065 ± 0.000	0.082 ± 0.000
	CLAP (Silva-Rodríguez et al., 2024)	2.01 ± 0.00	3.99 ± 0.01	2.31 ± 0.00	0.080 ± 0.000	0.060 ± 0.000	0.072 ± 0.000
UCF101	ZS	2.89 ± 0.01	5.24 ± 0.02	3.83 ± 0.01	0.124 ± 0.000	0.096 ± 0.000	0.124 ± 0.001
	ZSLP	1.58 ± 0.00	3.12 ± 0.01	1.98 ± 0.00	0.112 ± 0.000	0.074 ± 0.000	0.088 ± 0.000
	CoOp (Zhou et al., 2022b)	1.97 ± 0.01	3.12 ± 0.01	2.18 ± 0.01	0.114 ± 0.001	0.077 ± 0.000	0.110 ± 0.000
	KgCoOp (Hantao Yao, 2023)	1.74 ± 0.01	3.06 ± 0.01	2.06 ± 0.00	0.114 ± 0.001	0.070 ± 0.000	0.096 ± 0.000
	CLAP (Silva-Rodríguez et al., 2024)	1.63 ± 0.01	3.25 ± 0.01	2.00 ± 0.00	0.114 ± 0.001	0.076 ± 0.000	0.090 ± 0.000

Table 13: **Set size and CovGap** for CLIP (ViT-B) on 11 datasets across several few-shot adaptation approaches. Training for 16 shots.

		Set size (↓)			**CovGap** (↓)		
		LAC	APS	RAPS	LAC	APS	RAPS
Aircraft	ZS	18.70 ± 0.06	19.75 ± 0.06	20.74 ± 0.05	0.138 ± 0.000	0.139 ± 0.000	0.127 ± 0.000
	ZSLP	8.14 ± 0.03	9.56 ± 0.03	9.43 ± 0.04	0.079 ± 0.001	0.069 ± 0.000	0.082 ± 0.001
	CoOp (Zhou et al., 2022b)	7.19 ± 0.02	8.09 ± 0.02	8.88 ± 0.04	0.080 ± 0.001	0.070 ± 0.000	0.084 ± 0.001
	KgCoOp (Hantao Yao, 2023)	7.53 ± 0.02	8.72 ± 0.03	9.13 ± 0.04	0.080 ± 0.001	0.075 ± 0.000	0.084 ± 0.001
	CLAP (Silva-Rodríguez et al., 2024)	8.20 ± 0.03	9.59 ± 0.03	9.43 ± 0.04	0.079 ± 0.001	0.070 ± 0.000	0.083 ± 0.001
Caltech-101	ZS	0.94 ± 0.00	1.95 ± 0.01	1.20 ± 0.00	0.136 ± 0.001	0.092 ± 0.001	0.092 ± 0.001
	ZSLP	0.91 ± 0.00	1.12 ± 0.00	1.02 ± 0.00	0.151 ± 0.001	0.083 ± 0.001	0.082 ± 0.001
	CoOp (Zhou et al., 2022b)	0.91 ± 0.00	1.06 ± 0.00	1.02 ± 0.00	0.148 ± 0.001	0.084 ± 0.001	0.085 ± 0.001
	KgCoOp (Hantao Yao, 2023)	0.91 ± 0.00	1.19 ± 0.00	1.06 ± 0.00	0.150 ± 0.001	0.082 ± 0.001	0.083 ± 0.001
	CLAP (Silva-Rodríguez et al., 2024)	0.91 ± 0.00	1.22 ± 0.01	1.06 ± 0.00	0.146 ± 0.001	0.083 ± 0.001	0.085 ± 0.001
DTD	ZS	11.78 ± 0.06	13.30 ± 0.04	13.66 ± 0.06	0.122 ± 0.001	0.117 ± 0.001	0.121 ± 0.001
	ZSLP	2.91 ± 0.01	4.90 ± 0.03	3.34 ± 0.02	0.081 ± 0.001	0.071 ± 0.001	0.073 ± 0.001
	CoOp (Zhou et al., 2022b)	3.37 ± 0.02	4.50 ± 0.03	3.94 ± 0.04	0.084 ± 0.001	0.076 ± 0.001	0.081 ± 0.001
	KgCoOp (Hantao Yao, 2023)	3.53 ± 0.02	4.81 ± 0.03	4.04 ± 0.04	0.082 ± 0.001	0.073 ± 0.001	0.082 ± 0.001
	CLAP (Silva-Rodríguez et al., 2024)	3.03 ± 0.02	5.12 ± 0.03	3.48 ± 0.02	0.080 ± 0.001	0.069 ± 0.001	0.079 ± 0.001
EuroSAT	ZS	4.55 ± 0.01	4.78 ± 0.00	5.06 ± 0.01	0.103 ± 0.001	0.101 ± 0.001	0.102 ± 0.000
	ZSLP	1.46 ± 0.00	2.04 ± 0.00	1.84 ± 0.00	0.053 ± 0.000	0.045 ± 0.000	0.038 ± 0.000
	CoOp (Zhou et al., 2022b)	1.23 ± 0.00	1.59 ± 0.00	1.50 ± 0.00	0.041 ± 0.000	0.026 ± 0.000	0.031 ± 0.000
	KgCoOp (Hantao Yao, 2023)	1.28 ± 0.00	1.73 ± 0.00	1.61 ± 0.00	0.045 ± 0.000	0.032 ± 0.000	0.032 ± 0.000
	CLAP (Silva-Rodríguez et al., 2024)	1.53 ± 0.00	2.09 ± 0.00	1.90 ± 0.00	0.051 ± 0.000	0.044 ± 0.000	0.038 ± 0.000
Flowers-102	ZS	9.26 ± 0.05	9.52 ± 0.06	15.15 ± 0.08	0.180 ± 0.000	0.175 ± 0.000	0.179 ± 0.000
	ZSLP	1.03 ± 0.00	2.19 ± 0.01	1.58 ± 0.00	0.132 ± 0.001	0.087 ± 0.001	0.091 ± 0.001
	CoOp (Zhou et al., 2022b)	0.93 ± 0.00	1.30 ± 0.00	1.17 ± 0.00	0.094 ± 0.001	0.078 ± 0.001	0.078 ± 0.001
	KgCoOp (Hantao Yao, 2023)	0.93 ± 0.00	1.44 ± 0.01	1.24 ± 0.00	0.102 ± 0.001	0.079 ± 0.000	0.078 ± 0.001
	CLAP (Silva-Rodríguez et al., 2024)	1.09 ± 0.00	2.30 ± 0.01	1.65 ± 0.00	0.135 ± 0.001	0.089 ± 0.001	0.094 ± 0.001
Food-101	ZS	1.14 ± 0.00	1.89 ± 0.00	1.45 ± 0.00	0.054 ± 0.000	0.026 ± 0.000	0.031 ± 0.000
	ZSLP	1.08 ± 0.00	1.77 ± 0.00	1.39 ± 0.00	0.044 ± 0.000	0.023 ± 0.000	0.025 ± 0.000
	CoOp (Zhou et al., 2022b)	1.11 ± 0.00	1.64 ± 0.00	1.35 ± 0.00	0.050 ± 0.000	0.025 ± 0.000	0.030 ± 0.000
	KgCoOp (Hantao Yao, 2023)	1.08 ± 0.00	1.75 ± 0.00	1.38 ± 0.00	0.048 ± 0.000	0.022 ± 0.000	0.026 ± 0.000
	CLAP (Silva-Rodríguez et al., 2024)	1.07 ± 0.00	1.79 ± 0.00	1.39 ± 0.00	0.045 ± 0.000	0.023 ± 0.000	0.024 ± 0.000
ImageNet	ZS	2.81 ± 0.00	10.07 ± 0.02	3.23 ± 0.00	0.086 ± 0.000	0.069 ± 0.000	0.084 ± 0.000
	ZSLP	2.17 ± 0.00	6.60 ± 0.01	2.44 ± 0.00	0.076 ± 0.000	0.060 ± 0.000	0.074 ± 0.000
	CoOp (Zhou et al., 2022b)	2.39 ± 0.00	5.27 ± 0.01	2.73 ± 0.00	0.078 ± 0.000	0.064 ± 0.000	0.077 ± 0.000
	KgCoOp (Hantao Yao, 2023)	2.30 ± 0.00	5.95 ± 0.01	2.64 ± 0.00	0.078 ± 0.000	0.062 ± 0.000	0.077 ± 0.000
	CLAP (Silva-Rodríguez et al., 2024)	2.15 ± 0.00	6.85 ± 0.01	2.45 ± 0.00	0.077 ± 0.000	0.060 ± 0.000	0.074 ± 0.000
Oxford Pets	ZS	1.05 ± 0.00	1.43 ± 0.00	1.33 ± 0.00	0.109 ± 0.000	0.067 ± 0.000	0.072 ± 0.000
	ZSLP	0.94 ± 0.00	1.24 ± 0.00	1.17 ± 0.00	0.081 ± 0.001	0.040 ± 0.000	0.037 ± 0.000
	CoOp (Zhou et al., 2022b)	0.94 ± 0.00	1.16 ± 0.00	1.13 ± 0.00	0.083 ± 0.000	0.040 ± 0.000	0.041 ± 0.000
	KgCoOp (Hantao Yao, 2023)	0.94 ± 0.00	1.20 ± 0.00	1.15 ± 0.00	0.083 ± 0.001	0.038 ± 0.001	0.038 ± 0.000
	CLAP (Silva-Rodríguez et al., 2024)	0.95 ± 0.00	1.27 ± 0.00	1.19 ± 0.00	0.089 ± 0.001	0.039 ± 0.000	0.038 ± 0.001
Cars	ZS	2.24 ± 0.00	3.09 ± 0.01	2.49 ± 0.00	0.109 ± 0.000	0.080 ± 0.000	0.102 ± 0.000
	ZSLP	1.27 ± 0.00	1.98 ± 0.00	1.66 ± 0.00	0.082 ± 0.000	0.058 ± 0.000	0.057 ± 0.000
	CoOp (Zhou et al., 2022b)	1.37 ± 0.00	1.94 ± 0.00	1.66 ± 0.00	0.078 ± 0.000	0.057 ± 0.000	0.059 ± 0.000
	KgCoOp (Hantao Yao, 2023)	1.39 ± 0.00	2.04 ± 0.00	1.73 ± 0.00	0.080 ± 0.000	0.059 ± 0.000	0.061 ± 0.000
	CLAP (Silva-Rodríguez et al., 2024)	1.32 ± 0.00	2.04 ± 0.00	1.70 ± 0.00	0.080 ± 0.000	0.057 ± 0.000	0.057 ± 0.000
SUN397	ZS	2.83 ± 0.01	5.80 ± 0.01	3.21 ± 0.01	0.093 ± 0.000	0.073 ± 0.000	0.093 ± 0.000
	ZSLP	1.72 ± 0.00	3.49 ± 0.01	2.09 ± 0.00	0.075 ± 0.000	0.055 ± 0.000	0.063 ± 0.000
	CoOp (Zhou et al., 2022b)	1.87 ± 0.00	2.73 ± 0.00	2.04 ± 0.00	0.073 ± 0.000	0.060 ± 0.000	0.072 ± 0.000
	KgCoOp (Hantao Yao, 2023)	1.85 ± 0.00	2.91 ± 0.01	2.07 ± 0.00	0.076 ± 0.000	0.059 ± 0.000	0.070 ± 0.000
	CLAP (Silva-Rodríguez et al., 2024)	1.76 ± 0.00	3.55 ± 0.01	2.12 ± 0.00	0.075 ± 0.000	0.056 ± 0.000	0.064 ± 0.000
UCF101	ZS	2.89 ± 0.01	5.24 ± 0.02	3.83 ± 0.01	0.124 ± 0.000	0.096 ± 0.000	0.124 ± 0.001
	ZSLP	1.36 ± 0.00	2.85 ± 0.01	1.82 ± 0.00	0.106 ± 0.001	0.068 ± 0.000	0.077 ± 0.000
	CoOp (Zhou et al., 2022b)	1.51 ± 0.00	2.28 ± 0.01	1.76 ± 0.00	0.108 ± 0.001	0.068 ± 0.000	0.095 ± 0.000
	KgCoOp (Hantao Yao, 2023)	1.41 ± 0.00	2.47 ± 0.01	1.77 ± 0.00	0.106 ± 0.001	0.067 ± 0.000	0.081 ± 0.000
	CLAP (Silva-Rodríguez et al., 2024)	1.41 ± 0.00	2.94 ± 0.01	1.87 ± 0.00	0.108 ± 0.001	0.067 ± 0.001	0.079 ± 0.000